

**ANALYZING THE CONNECTIVITY POTENTIAL OF
LANDSCAPE GEOMORPHIC SYSTEMS: A RADAR REMOTE
SENSING AND GIS APPROACH, ESTUFA CANYON, TEXAS, USA**

A Dissertation

by

ELSAYED ALI HERMAS IBRAHIM

Submitted to the Office of Graduate Studies of
Texas A&M University
in partial fulfillment of the requirements for the degree of

DOCTOR OF PHILOSOPHY

August 2005

Major Subject: Geology

**ANALYZING THE CONNECTIVITY POTENTIAL OF
LANDSCAPE GEOMORPHIC SYSTEMS: A RADAR REMOTE
SENSING AND GIS APPROACH, ESTUFA CANYON, TEXAS, USA**

A Dissertation

by

ELSAYED ALI HERMAS IBRAHIM

Submitted to Texas A&M University
in partial fulfillment of the requirements
for the degree of

DOCTOR OF PHILOSOPHY

Approved by:

Chair of Committee,
Committee Members,

Head of Department,

John R. Giardino
Wyne Ahr
Vatche Tchakerian
Judith Chester
Christopher Mathewson
Richard Carlson

August 2005

Major Subject: Geology

ABSTRACT

Analyzing the Connectivity Potential of Landscape Geomorphic Systems: A Radar
Remote Sensing and GIS Approach, Estufa Canyon, Texas, USA. (August 2005)

ElSayed Ali Hermas Ibrahim, B.S., Mansoura University;

M.S., Mansoura University

Chair of Advisory Committee: Dr. John R. Giardino

Connectivity is considered one of the fundamental aspects that influences the rate of mass movement in the landscape. The connectivity aspect has been acknowledged from various conceptual geomorphic frameworks. None of these provided a developmental methodology for studying the connectivity of geomorphic systems, especially at the scale of the fluvial system. The emphasis in this research is placed on defining variables of the geomorphic systems that influence the connectivity potential of these systems. The landscape gradient, which is extracted from the Digital Elevation Model (DEM), and the surface roughness, which is extracted from radar images, are used to analyze the connectivity potential of geomorphic systems in the landscape. Integration of these variables produces a connectivity potential index of the various geomorphic systems that compose the fluvial system. High values of the connectivity potential index indicate high potential of the geomorphic system to transport mass whereas the low values indicate low potential of the geomorphic system to transport mass in the landscape. Using the mean values of the connectivity potential index, the

geomorphic systems in the landscape can be classified into geomorphic systems of low connectivity potential, geomorphic systems of intermediate connectivity potential and geomorphic systems of high connectivity potential. In addition to the determination of the relative connectivity potential of various geomorphic systems, the connectivity potential index is used to analyze the system-wide connectivity.

The ratios between the connectivity potential index of the upstream geomorphic systems and the connectivity potential index of the downstream geomorphic systems define system-wide connectivity in the landscape. High ratios reflect the high potential of the upstream geomorphic systems to transport mass in the downstream direction. Low ratios indicate the influence of the downstream geomorphic systems in maximizing mass movement in the upstream geomorphic systems. The presence of high and low ratios suggests the presence of a high system-wide connectivity. As the ratio approaches unity, mass movement is minimized in the landscape indicating low system-wide connectivity. Applying the above approach to Estufa Canyon, Texas, illustrated that Estufa Canyon is a dynamic fluvial system with high system-wide connectivity.

“Read!
In the Name of your
Lord
who has created all that exists”

Quran: Surat Al'alaq (Chapter 96): Verse (1)

ACKNOWLEDGMENTS

All kinds of praise and all thanks belong to ALLAH, the lord of the universe.

My gratitude and appreciation go to the Egyptian Government for sponsoring my family and me for five years.

My sincere thanks and respect go to Dr. Mohammad Adel Yahia, the former Chairman of the National Authority for Remote Sensing and Space Science, NARSS, Cairo, for his support, advice and encouragement.

I would like to express my thanks to my advisor, Dr. John R. Giardino for his advice and revision of this the dissertation. Special thanks to all my committee members, Dr. Ahr, Dr. Chester, Dr. Mathewson, and Dr. Vatche Tchakerian, for reviewing my dissertation.

I would also like to thank Ms. Farida Raghina, Radarsat Internatioanl, Ottawa, Canada, for her support fixing and getting the radar data in time.

Special thanks go to Dr. John Degenhardt for his time and effort during the fieldwork.

I would like to take this opportunity to thank my friend Mr. Abduallah Salmeen Bin Mahfouz for accompanying me during the second field trip. His companionship and patience in hot weather won't be forgotten.

TABLE OF CONTENTS

	Page
ABSTRACT.....	iii
DEDICATION.....	v
ACKNOWLEDGMENTS.....	vi
TABLE OF CONTENTS.....	vii
LIST OF FIGURES.....	ix
 CHAPTER	
I INTRODUCTION.....	1
Introduction.....	1
Problem Statement.....	3
Objective.....	4
Justification.....	4
Description of the Dissertation.....	5
II LINKED GEOMORPHIC SYSTEMS.....	7
Introduction.....	7
General System Theory.....	7
Literature Review.....	9
Conceptual Basis for Analyzing the Connectivity Potential of Geomorphic Systems.....	15
Landscape Gradient.....	16
Surface Roughness.....	19
Radar Imagery.....	20
III STUDY AREA.....	25
Introduction.....	25
Climate.....	25
Geology.....	30
Rock Types.....	30
Tectonics.....	38
Soil.....	39

CHAPTER	Page
Vegetation.....	40
Geomorphology.....	44
The Western Terrain.....	44
The Eastern Terrain.....	46
IV DATA DESCRIPTION AND STUDY METHODOLOGY.....	51
Introduction.....	51
Data Acquisition and Description.....	53
Digital Elevation Model.....	53
Digital Orthophotos Qaudrangle (DOQ).....	53
Radarsat Images.....	54
Digital Image Processing.....	57
Mosaicking the Digital Orthophoto Images.....	57
Extracting Radar Backscattering Coefficient.....	58
Speckle Reduction.....	61
Data Geocoding.....	62
Extracting Thematic Layers.....	65
Data Geocoding.....	66
Data Analysis.....	67
V DATA ANALYSIS.....	69
Introduction.....	69
Geomorphic Systems of Estufa Canyon.....	69
The Landscape Gradient.....	73
The Surface Roughness.....	78
Data Integration.....	84
Analyzing the Connectivity Potential of the Geomorphic Systems.....	90
System-Wide Connectivity.....	96
VI CONCLUSION AND FUTURE DIRECTIONS.....	103
Conclusion.....	103
Future Directions.....	108
REFERENCES.....	111
VITA.....	118

LIST OF FIGURES

FIGURE	Page
1 The main components of the morphologic and the cascading system are shown together.....	10
2 A diagram showing the detachability continuum.....	23
3 Location map of Estufa Canyon, Big Bend National Park, Texas.....	26
4 Average monthly distribution of rainfall over Panther Junction and and Chisos Basin, Big Bend National Park, Texas.....	28
5 The distribution of the average monthly temperature over a period extending from 1948 to 2001 at Chisos Basin and Panther Junction climatic stations, Big Bend National Park, Texas.....	29
6 The diurnal variation at both Chisos Basin and Panther Junction stations, Big Bend National Park, Texas.....	31
7 Rock disintegration in the high gravel terrace of the study area.....	32
8 Geologic map of Estufa Canyon.....	35
9 Igneous rocks in the western part of Estufa Canyon and Quaternary unconsolidated deposits.....	36
10 Holocene alluvial deposits flanked by a high terrace of Neogene gravel.....	37
11 Soil map of Estufa Canyon.....	41
12 Vegetation cover of Estufa Canyon.....	43
13 The main geomorphic units of Estufa Canyon.....	47

FIGURE	Page
14 A flow chart showing the methodology of studying the connectivity potential of geomorphic systems.....	52
15 A drawing shows the geometry involved in a sideways-looking radar-imaging system.....	56
16 The origin of speckle in radar imageries.....	63
17 An example shows a Radarsat-1 image before removing the speckle (A) and after removing the speckle (B).....	64
18 Main geomorphic systems of Estufa Canyon.....	70
19 The landscape gradient of Estufa Canyon.....	74
20 A graph showing the rate of changes in the landscape gradients in the downstream direction of Estufa Canyon.....	77
21 A graph showing the relationship between the size of the object, wavelength, and intensity of backscattering.....	82
22 A Radarsat-1 image showing the variation of the backscattering over various roughness surfaces.....	85
23 The relationship between the landscape gradient and the particle size distribution in the downstream direction.....	87
24 The relationship between radar backscattering and the landscape gradient...	89
25 A map showing the spatial variation in the connectivity index of Estufa Canyon.....	92
26 The connectivity potential index of various geomorphic systems in	

FIGURE		Page
	Estufa Canyon.....	95
27	The relationship between the potential energy and system dynamic.....	98
28	The interaction between various geomorphic systems in Estufa Canyon.....	100

CHAPTER I

INTRODUCTION

Introduction

Landscapes are composed of various geomorphic systems. In the downstream direction, mass movement takes place from one system to another system through various spatial links. The rate of mass movement through geomorphic systems is a function of the frequency and magnitude of external forces along with internal forces. External forces include climate, sea level and tectonic movement. In addition to the influence of the external forces, a fundamental aspect that controls the rate of mass movement in the landscape is the connectivity potential of various geomorphic systems.

The connectivity aspect of geomorphic systems can be studied from various perspectives by earth scientists. These perspectives focused on the role of connectivity in fluvial systems and on the mechanisms by which the connectivity between geomorphic systems operates. The role of connectivity in the fluvial system relates to the process interaction between various geomorphic systems. These process interactions control the intensity of mass movement in the downstream direction. In addition, the transmission of changes in the upstream direction that occurs in response to external environmental perturbations, such as sea level changes; illustrate the influence of the connectivity on the upstream propagation of these changes. In this theme, various theoretical frameworks have been established to understand the process interaction of geomorphic systems in response to environmental perturbations. Among these concepts are the process linkage

This dissertation follows the style of Geomorphology.

and complex response. Another theme of studying the connectivity between the geomorphic systems focuses on the mechanisms by which various geomorphic systems are connected. In this perspective, the geomorphic systems are considered as physical entities that are linked by various spatial links. These links include lines (e.g., stream channels), points (e.g., outlets), boundaries (e.g., edges), and polygons (e.g., a geomorphic system that connects two different geomorphic systems). Through the spatial links, mass transmission takes place. The higher the potential of the spatial link to transmit mass, the higher the connectivity is between geomorphic systems. The two themes, the role of the connectivity and the mechanism of the connectivity, can be studied using various conceptual frameworks. Whereas the process linkage concept (Ritter et al. 2002) and the complex response concept (Schumm 2003) focus on connectivity from the process interactions between various geomorphic systems, the coupling concept (Brunsden and Thornes 1979) placed an emphasis on the spatial links that connect geomorphic systems.

Although these concepts have been proposed for the study of the connectivity between geomorphic systems and their role in controlling mass movement in the landscape, few studies have been carried out to develop these concepts, especially at the scale of the fluvial system. In this dissertation, the connectivity aspect of geomorphic systems was studied from a different view. In this view, the focus is placed on studying the connectivity potential of various geomorphic systems in the landscape. The connectivity potential can be defined as the potential of the geomorphic system to transport mass to another geomorphic system. The connectivity potential can be studied

as a function of the magnitude and the spatial variabilities of important variables of geomorphic systems. The geomorphic system that has high connectivity potential is characterized by a high potential for mass transmission whereas the geomorphic system that has low connectivity potential is characterized by a low connectivity potential for mass transmission. Determining the relative connectivity potential can contribute to the understanding of system wide connectivity that controls the overall potential of the fluvial system for mass movement. To accomplish this, two variables of the geomorphic systems were used: a topographic variable and a physical variable. The topographic variable is represented by the landscape gradient whereas the physical variable is represented by the surface roughness. Both of the variables were integrated in the analysis using Geographic Information Systems (GIS) functions and operations to analyze the connectivity potential of various geomorphic systems and system wide connectivity of the whole fluvial system.

Problem Statement

Connectivity is a fundamental aspect of geomorphic systems. This aspect controls the intensity of mass movement in the landscape. Although various studies have been introduced to discuss the connectivity between geomorphic systems (Ritter et al. 2002, Brunnsden and Thornes 1979 and Schumm 2003), these studies all have been more or less theoretical or they were limited to small-scale applications, such as hillslopes. Unfortunately, none of these studies provided a methodological framework for measuring and analyzing the connectivity potential of geomorphic systems especially at

the fluvial system scale. In this dissertation, a methodology for developing the connectivity potential is introduced to define, map, and evaluate the connectivity potential of various geomorphic systems using the radar remote sensing imagery and GIS.

Objectives

Seven objectives have been established to address the problem of this dissertation.

- Define and map geomorphic systems in the study area based on lithologic and topographic homogeneity;
- Extract the landscape gradient of the study area from a Digital Elevation Model;
- Map the surface roughness of the study area using Radarsat-1 imagery;
- Produce a connectivity potential index (CPI) image by the integration of the surface roughness and the landscape gradient;
- Develop a mean connectivity potential index for each geomorphic system using the image of the connectivity potential index;
- Classify the connectivity potential of the geomorphic systems into low, intermediate and high;
- Evaluate system-wide connectivity.

Justification

Geomorphic landscapes represent the backdrop for all human activities and ecosystems. Geomorphic systems that form these landscapes are spatially and temporally

dynamic. All are connected at various levels. A change in a geomorphic system in response to environmental perturbations can trigger subsequent changes in other geomorphic systems of the landscape. The trend and the strength of the response of geomorphic systems to environmental perturbations depend, to a large extent, on the connectivity potential of various geomorphic systems that form the landscapes. Determining the connectivity potential of various geomorphic systems can help understand and predict the magnitude and trends of possible future changes in the landscape in response to the forecasted environmental perturbations. This understanding can provide the decision makers and landscape managers with useful information for conserving natural resources and establishing a successful strategy for future development.

Description of the Dissertation

This dissertation presents a new perspective for defining and mapping connectivity potential of geomorphic systems. In addition to this introduction, five chapters have been written to fulfill the objectives of the study and to answer the problem statement.

Chapter II is a review of previous work that has been introduced. In this review, an overview of the applications of the system concept in geomorphology is discussed. The interconnection between various geomorphic systems from the process domain is reviewed through presenting various concepts such as process-linkage, complex response, and coupling. Finally, various aspects of the connectivity phenomenon in the

landscape were introduced. A conceptual framework for developing a methodology to study and analyze connectivity potential is presented in this chapter, also.

Chapter III presents the area of the study where the methodology of studying connectivity potential was applied. The study area is Estufa Canyon, Big Bend National Park, Texas, USA. The climate, geology, tectonics, soil, and vegetation along with geomorphic characteristics of Estufa Canyon are discussed.

Chapter IV describes the data and the methodology used to develop the connectivity potential. Data acquisition and specifications are presented. The detailed steps of the digital image processing, the methods of thematic map extraction, the data integration, and the data analysis are introduced.

Chapter V presents the results of data analysis. The characteristics of the landscape gradient and the surface roughness in the study area are described. The integration of the surface roughness and the landscape gradient is discussed. The process of analyzing the connectivity potential index of geomorphic systems is introduced. System-wide connectivity concept is introduced in this chapter, also.

Chapter VI presents a conclusion to the study. The conclusion includes the main results of addressing the objectives that were established to answer the problem stated in the first chapter of the dissertation.

CHAPTER II

LINKED GEOMORPHIC SYSTEMS

Introduction

Geomorphic landscapes represent the backdrop for all the activities that occur on Earth. These landscapes, which can be considered as systems, are composed of various geomorphic subsystems. Each subsystem has a boundary, inputs/outputs, regulators, pathways and storage of mass and energy. The output of energy and mass from one geomorphic system is transported to another geomorphic system through various pathways and spatial links. One of the fundamental aspect that controls the intensity of mass movement from one geomorphic system to another geomorphic system is the connectivity potential of these systems. The connectivity concept focuses on the potential of a geomorphic system to transport mass and energy from one location to another location within the landscape. The concept of a system can be approached from various perspectives. In this chapter, a review of General System Theory and its applications in geomorphology, a discussion of various concepts of the connectivity aspect between geomorphic systems, the conceptual bases for studying connectivity potential of geomorphic systems are discussed.

General System Theory

General System Theory was proposed by Ludwig Von Bertalanffy (1956). In this theory, a physical entity is considered as a system composed of various elements that can

interact with each other to perform a specific process within the whole system. Chorley (1962) introduced the concept of General System Theory into geomorphology as a structural framework to consider the interaction, flow and storage of energy and mass through a defined area. Using this approach, a landscape can be considered to be composed of geomorphic systems. Each system has a boundary, inputs/outputs, regulator, pathways, and storage of mass and energy. Components of the systems are characterized by interdependency (Huggett 1985 and Chorley and Kennedy 1971). Chorley and Kennedy (1971) provided an elaborate investigation of the structural framework of the system.

Based on the internal structural complexity of a geomorphic system, Chorley and Kennedy (1971) defined three hierarchical internal systems within each geomorphic system. These systems are the morphologic system, the cascading system and the process response system. A morphologic system is composed of components and their attributes (Fig. 1). System components include lithology, slopes, landforms, vegetation, soil, etc. Each component has various attributes such as structure, composition, and texture. As a system, components and their attributes should have some degree of interconnections (Chorley and Kennedy 1971, and Phillips 1992, 1999).

The interconnection between various morphologic systems controls mass movement of cascades such as water and debris flows. Generally, the morphologic systems form the vessels of the cascading system. Cascading systems are the structures within which the input and the output of mass and energy move (Chorley and Kennedy 1971); the structure of the cascading system includes the regulators as well (Fig. 1). The

regulator controls the diversion of energy and/or mass either to store the input of the energy and/or mass or to form the throughput producing system output. The interaction between the morphologic and the cascading systems form the process-response system (Chorley and Kennedy 1971). This interaction is represented by mutual adjustments in the morphologic components (i.e., the response) as a result of the dynamic nature of the cascades (i.e., the process). Whereas the interaction between system morphology and system cascade controls the system output, the connectivity potential of the geomorphic systems controls the rate and intensity of mass movement within a landscape.

The connectivity aspect has been acknowledged using various concepts in geomorphology such as system coupling (Brunsden and Thornes 1979), process linkage (Ritter et al. 2002), and complex response (Schumm 2003). These concepts acknowledge the connectivity between geomorphic systems from various perspectives.

Literature Review

“Everything that happens in, on, to, or near the surface of the Earth is connected, directly or indirectly, to everything else” (Phillips 1999: 1). Because of this connection, a change in the external forces results in a series of changes in the geomorphic systems of the landscape. Ritter et al. (2002) proposed the “Process Linkage” concept to express the domino effect of altered external conditions on the geomorphic systems. A single change in a geomorphic system as a response to an external environmental change can trigger totally different geomorphic processes in the linked geomorphic systems of the landscape. Another concept that has been introduced into geomorphology to express the

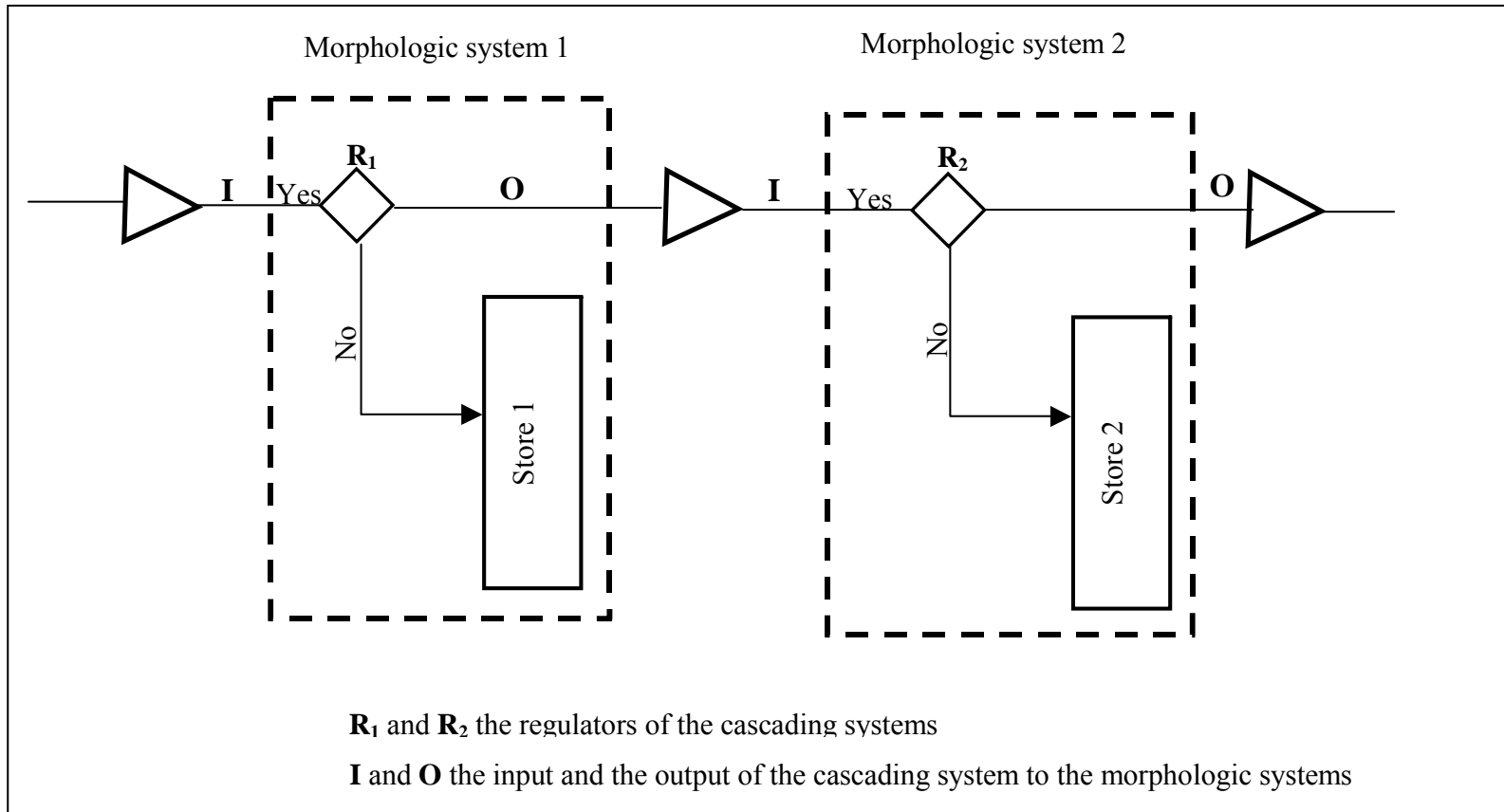


Fig. 1: The main components of the morphologic and the cascading system are shown together (modified after Chorley and Kennedy 1971).

interconnection between geomorphic processes in a system as a result of environmental perturbations is the complex response (Schumm 2003).

The concept discusses the complex response of geomorphic system components to environmental perturbations such as climate, base level, or tectonic changes. The complex response is composed of a sequence of erosional and depositional events that occurs in a geomorphic system as a result of environmental perturbations. For example, following uplift, the main stream channel is incised to form a terrace in the alluvial plain. Incision occurs first at the mouth of the main basin and then a progressively upstream headward incision results in scouring of the alluvial plain. At this temporal point, the main channel becomes more powerful and can transport upstream deposits in the downstream direction in large quantities. Continuous transportation results in deposition and formation of a braided stream. The full process is repeated again in response to another period of uplift (Schumm 2003). The complex-response concept focuses on the linkage between various geomorphic processes and the equivalent adjustments in the stream channel and alluvial plain.

Harvey (1994, 2001) studied the effect of coupling of seasonal process interactions on eroding hillslope gullies. In this study, the relationships between slope processes and basal streams are considered to be controlled by the coupling zone. Strong coupling occurs where erosion rates and sediment accumulation decline. Weak coupling occurs where erosion rates on the hillslopes increase, resulting in high sediment accumulation. The first case permits high sediment transmission whereas the second case suppresses sediment transmission from the hillslope to the basal stream. Humphrey

and Heller (1995) modeled the influence of a single perturbation on a coupled fluvial system. A single perturbation of an external force such as a change in rainfall, base level, or tectonic activity produces dampened, long-term internal oscillations. The oscillations occur as a series of cutting and filling processes throughout the fluvial system. The highest magnitude of oscillations takes place at the coupling point between the highly erosive mountainous areas and the depositional fluvial basins.

The above-mentioned studies mainly focus on the connectivity between the geomorphic systems from the perspective of the process interrelationship using various conceptual frameworks. Using that perspective, a single change in a geomorphic system as a result of external perturbation can trigger a series of changes in other geomorphic systems. None of these concepts address the potential of various geomorphic systems to transmit mass and energy through a landscape. Brunsdon and Thornes (1979) introduced the concept of coupling between geomorphic systems to describe various spatial links between geomorphic systems and their possible influence on process interactions.

Brunsdon and Thornes (1979) introduced the concept of coupling between the geomorphic systems in the context of discussing landscape sensitivity to change. The coupling concept was introduced as an aspect of the geomorphic system resistance to environmental changes. Brunsdon (1993) demonstrated the coupling linkage between geomorphic systems in more detail. According to the type of coupling linkages between geomorphic systems, Brunsdon (1993) identified three coupling linkages: not coupled linkage, coupled linkage, and decoupled linkage. The classification depends on the mechanism by which the geomorphic systems are spatially connected. In not coupled

geomorphic systems, there is a boundary between geomorphic systems but no mass and energy passes through boundary. In coupled linkage, the transmission of mass and energy occurs between geomorphic systems that are spatially linked through a boundary, a joint, or a link. In decoupled linkages, two geomorphic systems are temporally separated by another geomorphic system. Studying the connectivity between geomorphic systems from this perspective sets the stage for studying the spatial connectivity between geomorphic systems and their influence on process connectivity. Jones (2000) presented various types of spatial links by which sediments are transferred between sediment stores within mountain basins. He described conduits as parts of the main river system (such as alluvial fans) or as parts of the tributary system (as alluvial channels). These conduits and paths act to transfer sediment between various sediment stores within mountainous basins.

Reviewing the previous literature that approaches the connectivity aspect in the landscape, it is possible to identify two types of connectivity: process connectivity and spatial connectivity. The first focuses on the process interaction that takes place between various geomorphic systems. The second, which is the spatial connectivity, places an emphasis on the mechanisms by which various geomorphic systems are connected such as lines, points, areas and boundaries. Both the process connectivity and the spatial connectivity, as important aspects of the landscape, still need to be studied in more detail regarding their role in controlling the rate of mass movement in the landscape at various time and spatial scales. Limited studies have recently been conducted to apply the connectivity concept for understanding various phenomena in the landscape.

Gilvear (1999) described various factors affecting river engineering in fluvial systems; he identified the longitudinal and lateral connectivity in fluvial systems. The longitudinal connectivity expresses the variations in the downstream hydraulic connectivity. In this aspect, upstream impacts spread temporally in the downstream direction resulting in longitudinal connectivity. The lateral connectivity addresses the interrelationships between channel streams and the floodplains. Floodplain inundation dissipates energy during floods whereas confinement between embankments results in higher stream power. Poole et al. (2002) studied the influence of the surface and the subsurface geomorphic structures of the floodplain for facilitating the hydraulic connectivity between the channel and the floodplain. Croke et al. (in press) defined two types of connectivity: direct connectivity via channels or gullies and diffuse connectivity via pathways. The first, direct connectivity, occurs as a result of gully pathways whereas the second, diffuse connectivity, occurs in dispersive channels. These kinds of studies need to be extended for understanding the role of the connectivity aspect not only between the contiguous geomorphic systems at local scales but also between various distant geomorphic systems at the scale of the whole drainage basins.

This dissertation will build on these studies. The focus is placed on analyzing connectivity potential of geomorphic systems in the landscape. The analysis is based on using important variables that affect the connectivity potential of the geomorphic systems. These variables include a topographic variable and a physical variable. The topographic variable is represented by the landscape gradient whereas the physical variable is represented by the surface roughness. Both of these variables can be used to

identify, map and evaluate the connectivity potential of various geomorphic systems in the landscape.

Conceptual Basis for Analyzing the Connectivity Potential of Geomorphic Systems

Landscapes are temporally and spatially dynamic. The dynamic nature of landscapes is a function of various external and internal variables. External variables include climate, tectonic, and sea level changes. Internal variables include geology, vegetation and topographic characteristics. Along with these variables, time is an important variable that should be taken into account in studying landscape dynamics. The relationship between the dynamic of landscape and external and internal variables can be expressed as follows:

$$\text{Landscape} = f(\text{time, tectonic, climate, sea level changes, geology, relief, vegetation, etc.})$$

In studying the connectivity potential of geomorphic systems, attention was paid to the potential of geomorphic system to transport mass from one geomorphic system to another a geomorphic system. The gravitational force that is dominant in the geomorphic system is considered one of the most important variables that affect the rate of mass movement. The relief that is produced by uplift or by erosional processes determines the gravitational forces acting on the geomorphic system (Schumm 2003). One of the relief characteristics that control the gravitational force is the slope. The slope represents a

fundamental variable that can be used to study the connectivity potential of a geomorphic system in the landscape. Another factor that affects mass movement in geomorphic systems is the physical characteristics of slopes in the geomorphic systems. These physical characteristics include grain size and vegetation. In arid and semi-arid environments, the influence of vegetation on geomorphic processes is limited when compared to its influence in humid environments. The spatial variations in particle size distribution are more significant in determining the potential of geomorphic systems for mass movement. The rate and the intensity of water movement and mass movement in the landscape are functions of slope and the textural properties of materials forming the landscape (Etzelmuller 2000).

In this dissertation, the focus is placed on the connectivity potential of various geomorphic systems in the landscape. The connectivity potential of a geomorphic system expresses the ability of a geomorphic system to transport mass and energy in the landscape. The highly connective geomorphic system is the system that has a high potential to transport mass in the landscape and vice versa. To address this connectivity aspect from this view, the landscape gradient and the surface roughness have been integrated to develop a connectivity index that expresses the connectivity potential of the geomorphic systems in the landscapes.

The Landscape Gradient

Slope is one of the most important topographic parameters in the landscape (Mark 1975). Slope controls the gravitational forces that are responsible for the

geomorphic work in the landscape. To study the influence of slope on the connectivity potential of geomorphic systems, the magnitude, the spatial distribution, and the amount of changes of slopes are considered important characteristics of the landscape gradient to determine the relative connectivity potential of geomorphic systems in the landscape.

Scholz (1972) identified various slope classes according to slope magnitude. These classes include plain ($0.0 - 0.5^\circ$), slightly slopping ($0.5 - 2.0^\circ$), gently inclined ($2.0 - 5.0^\circ$), strongly inclined ($5.0 - 15.0^\circ$), steep ($15.0 - 25.0^\circ$), very steep ($25.0 - 35.0^\circ$), precipitous slopes ($35.0 - 55.0^\circ$), and vertical slopes ($> 55.0^\circ$). Various geomorphic processes and landforms characterize each slope class. The potential of mass movement, basically, depends on the magnitude of the dominant slope class in the geomorphic system. The higher the magnitude of the dominant slope in a geomorphic system, the higher the connectivity potential. In addition to the magnitude of the dominant slope in the geomorphic system, the spatial distribution of the slope in the landscape plays a critical role in determining the spatial variabilities of the connectivity potential of the geomorphic system through various landscape systems such as the fluvial system.

In the ideal fluvial system, high slopes characterize the watershed areas whereas the low slopes characterize the alluvial plains at the outlets. In reality, alternating various slope classes occur through a fluvial system on a random basis. For instance, the watershed areas of high slopes may be flanked downstream by a slightly slopping pediment surface that might be flanked again by steep slopes. This complex nature of the spatial variabilities of the slope affects the connectivity potential of geomorphic systems.

In addition, the magnitude of changes of the slope from one geomorphic system to another geomorphic system influences the intensity of mass movement in the landscape. The higher the difference of the magnitudes of the slopes between various geomorphic systems, the higher the connectivity potential between various geomorphic systems in the landscape. Studying the magnitude, the spatial distribution and the changes of the slopes between various geomorphic systems can help in the understanding of the connectivity potential. To study the relationship between the slope characteristics and the connectivity potential of a geomorphic system, a direct proportional relationship between the slope magnitude (S) and the connectivity potential (C_p) is suggested as:

$$C_p \propto S \quad (1)$$

Thus,

$$C_p = K_1 * S \quad (2)$$

where:

C_p is the connectivity potential of the geomorphic system,

S is the mean slope of the geomorphic system, and

K_1 is the proportional constant that includes all other system parameters such as geology, vegetation, and surface roughness.

Along with various slope characteristics, the physical characteristics of the slope surfaces influence the connectivity potential of the landscape. These characteristics involve the surface roughness.

Surface Roughness

Surface roughness, from a topographic point of view, expresses the elevational irregularities of a topographic surface (Mark 1975, Etzelmuller 2000). Mark (1975) defined two topographic expressions of surface roughness: grain and texture. The grain topographic surface is the surface that has the longest significant wavelengths of elevational variations over the surface, such as ridges and valleys. Texture represents the shortest significant topographic wavelengths between the grains in the landscape. Recently, centimeter-scaled variations of the topography, which are known as micro-topography or microscale topography, have been studied using various remote sensing imageries such as Radarsat-1 satellite imagery (Shaber et al. 1976, Brown 1987, Wall and Farr 1991). Along with slope magnitude, these fine-scale topographic variations can be used to analyze the connectivity potential of geomorphic systems.

The surface roughness concept is widely used in different disciplines. For example, in oceanography, the surface roughness is used to express the variations of ocean wave heights. In radar remote sensing applications, the surface roughness concept is widely used to express the roughness of various surfaces such as forests, ocean surface, and soil surfaces. In geomorphology, surface roughness mostly refers to the topographic irregularities of a terrain surface (Mark 1975, Pike and Rozema 1975, Etzelmuller and Sulebak 2000). In this dissertation, the surface roughness is used to evaluate the textural variabilities over the study area as a result of granular variations of various slope surfaces. Radar remote sensing imagery is used along with fieldwork and

supplementary data such as soil survey data to analyze the textural characteristics of the landscape and its role in the connectivity potential of the geomorphic systems.

Radar Imagery

Radarsat-1 imagery is produced by microwave satellites. The Radatsat-1 satellite operates in the microwave frequency known as “C” band (5.3 GHZ frequency or 5.6 cm wavelength). These satellites transmit and receive the energy in a horizontal polarization (HH polarization). Radarsat-1 satellite acquires images at various beam modes (spatial resolution). The fine beam modes produce images of 6 – 8 meter spatial resolution. Variations of the returned signal (the radar backscattering) are the result of changes in the surface roughness, moisture content, and the electrical property of the surface. The fine beam mode, horizontal polarization and appropriate incident angles along with the short wavelengths provide the capabilities to record the backscatter that is dependant on the *centimeter-scale surface roughness* (Radarsat International 1997). With this level of accuracy, surface roughness of the study area can be evaluated.

Radarsat-1 images are used to discern surfaces based on surface roughness. High backscatter values indicate a rough surface whereas low backscattering values imply a fine surface. Rough surfaces are attributed to coarse textured surfaces. Fine surfaces are attributed to fine textured surfaces. Rough surfaces normally occur in high elevations and have steep slopes whereas fine surfaces occur in lower elevations and have low slopes. A surface of high elevation and with a steep slope (high surface roughness) is characterized by a high potential for mass movement. A surface of low elevation and a

gentle slope (low surface roughness) is characterized by a low potential for mass movement. A relationship between the surface roughness (F) and the connectivity potential of a geomorphic system (C_p) is suggested. Thus, rough surfaces indicate a high potential of connectivity and fine surfaces indicate a low potential of connectivity. Therefore, this relationship is expressed as:

$$C_p \propto F \quad (3)$$

Thus,

$$C_p = K_2 * F \quad (4)$$

where:

C_p is the system connectivity,

F is the surface roughness, and

K_2 is a constant that include other system parameters.

Combining equations (2) and (4) produces an index that expresses wide range of spatial variations in both the slope and the surface roughness. Assuming a common constant (K) for a geomorphic system, which represents others parameters in the geomorphic systems such as lithology, vegetations, moisture, etc. The connectivity potential of a geomorphic surface can be represented as:

$$C_p = K * S * F \quad (5)$$

In this equation, high values of the C_p indicate the presence of areas of high slopes and high surface roughness (coarse materials) whereas low values of C_p indicate the presence of areas of low slopes and fine debris. However, the relationship between the surface roughness and the slope is various and depends on various geologic conditions. Although the common relationship shows a direct positive correlation between the slope and the surface roughness, some exceptions take place. For instance, a bare source rock of steep slope might occur where the surface roughness, as a function of particle size, is minimum or zero (Fig. 2). In this case, the C_p is zero while the slope is steep. To overcome this, the equation can be written in this form:

$$C_p = K * S * (1 - F) \quad (6)$$

The index can be developed using various raster GIS operations. In these operations, an image that represents the slope (S) and another image that represents the surface roughness (F) are combined together to produce an image that expresses the connectivity potential index. The lower values of the produced image represent locations that have the lowest values of the slope and the lowest values in the surface roughness. These locations have low connectivity potential for transporting mass in the landscape. The high values in the image represent areas that have the highest values of the slopes and the surface roughness. These locations have the highest potential for mass movement and then a high connectivity potential. Between these extremes, a wide range

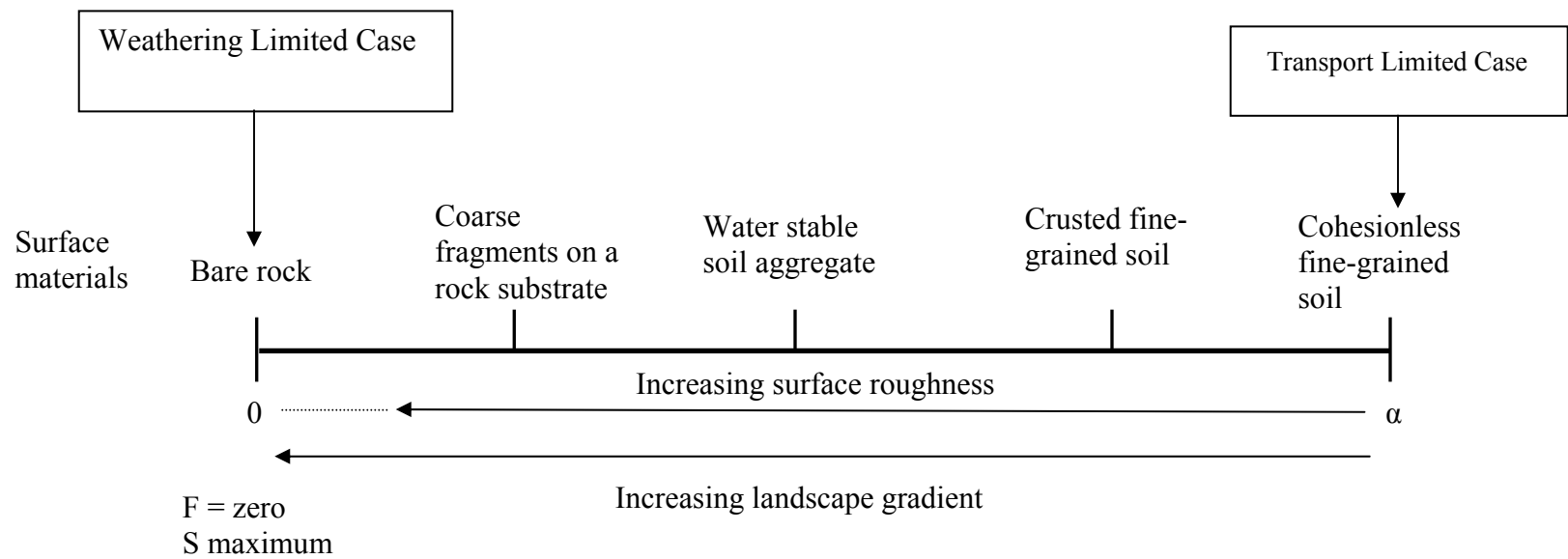


Fig. 2: A diagram showing the detachability continuum (modified after Parsons 1988).

of indices occurs reflecting high spatial variabilities in the connectivity potential of various geomorphic systems in the landscape. Using this wide range of the connectivity potential, a classification of the geomorphic systems based on their relative connectivity potentials can be carried out to define geomorphic systems of low, medium and high connectivity potentials. Wide system connectivity can be evaluated as well.

CHAPTER III

STUDY AREA

Introduction

The study area for this dissertation is the drainage basin of the Estufa Canyon, Big Bend National Park, Texas. The park is accessed by State Road 385 from Marathon, Texas. Estufa Canyon drainage basin is located south of the Park headquarters. The canyon extends from the Chisos Mountains in the west to Tornillo Creek in the east. Geographically, the study area extends from 103° 04' W to 103° 13' W and from 29° 16' N to 29° 20' N (Fig. 3). The Estufa Canyon occupies an area of ~ 35 km².

Climate

Climate is one of the main driving forces of geomorphic processes in the landscape (Ritter et al. 2002). Each climatic zone is characterized by dominant climatic parameters such as precipitation and temperature. Arid to semi-arid climates dominate Big Bend National Park. In these climates, the rate of evaporation exceeds the rate of precipitation. Two climatic stations are located close to the study area: one at Panther Junction and another one at Chisos Basin. Climate records have been obtained from the Park (National Weather Service). The climate records cover the time period extending from 1957 to 2001 for precipitation data and from 1948 to 2001 for temperature data. Understanding temporal and spatial variations of climatic parameters aid in the evaluation of dominant geomorphic processes in the landscape.

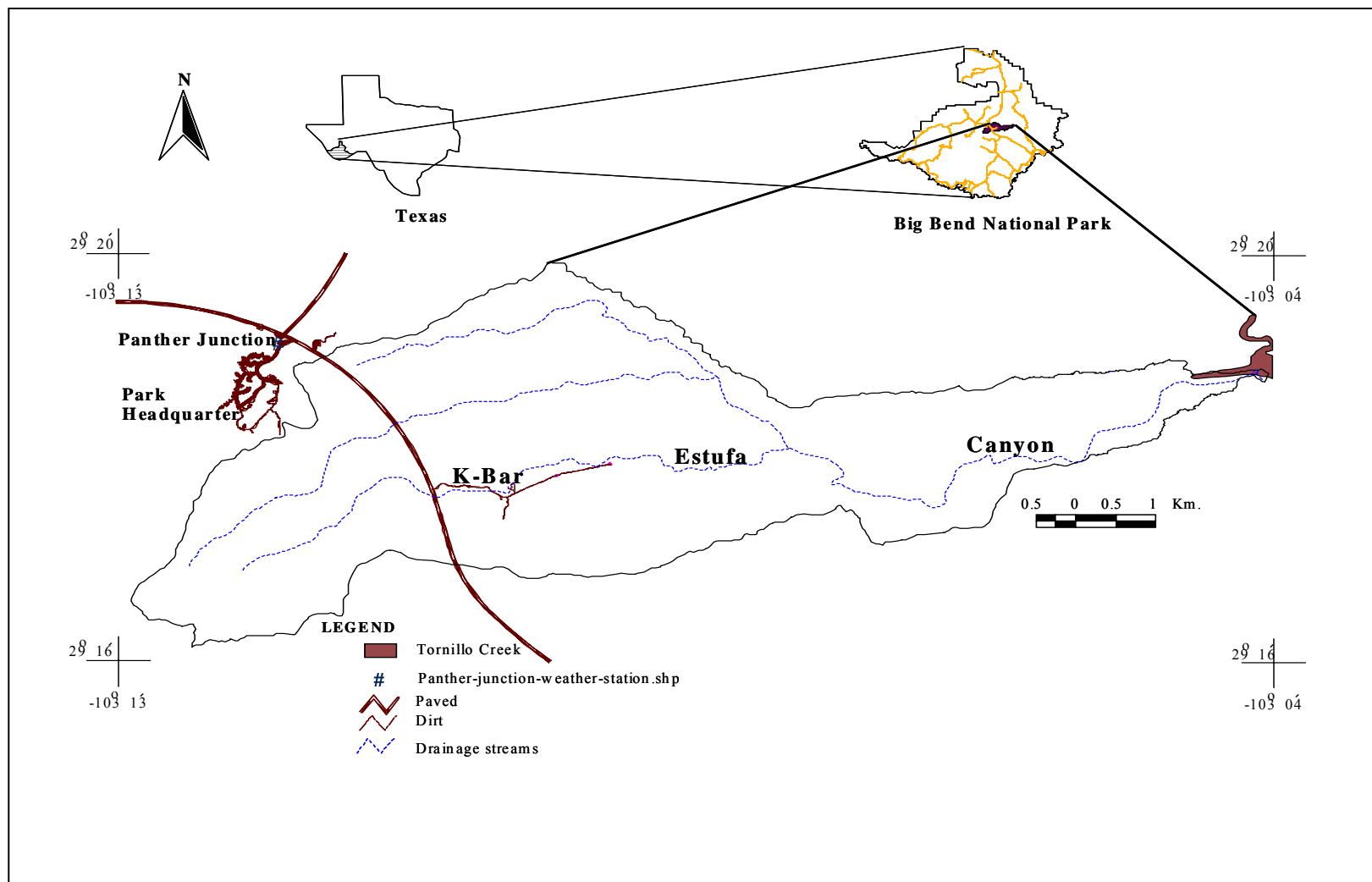


Fig. 3: Location map of Estufa Canyon, Big Bend National Park, Texas.

The analysis of climatic data shows that the total annual precipitation is 34.80 cm at Panther Junction and 47.00 cm at Chisos Basin. Precipitation is higher in the summer than in the winter (Fig. 4). The highest monthly precipitation is recorded in July and August where the average monthly precipitation is higher than 5.00 cm. The lowest values are recorded in March, February, January, December, and November where the average monthly precipitation is lower than 1.50 cm. This temporal distribution of precipitation is responsible for producing flash floods in summer months. Flash floods are characterized by intense surface runoff and transportation of mass through geomorphic systems from high to low elevations. Besides precipitation, daily and monthly variations in temperature have a considerable potential of producing debris in the landscape.

Data records of temperature show that the average temperature ranges from 9.60° C to 18.83° C at Panther Junction, and from 8.13° C to 16.72° C at Chisos Basin in winter. In summer, the monthly average temperature ranges from 19.45° C to 27.27° C at Panther Junction and from 23.47° C to 29.65° C at Chisos Basin. The lowest values are recorded in January and December whereas the highest values are recorded in June, July, and August (Fig. 5). The high variability of temperature among months discloses seasonal temperature variations. In addition to seasonality in temperature changes, diurnal changes are also considerable. Diurnal changes at Panther Junction are higher than at Chisos Basin (Fig. 6). This difference might be attributed to elevation changes (1,121 m for Panther Junction and 1,606 m for Chisos Basin). The highest diurnal changes occur in the spring months (March, April and May) whereas the lowest diurnal

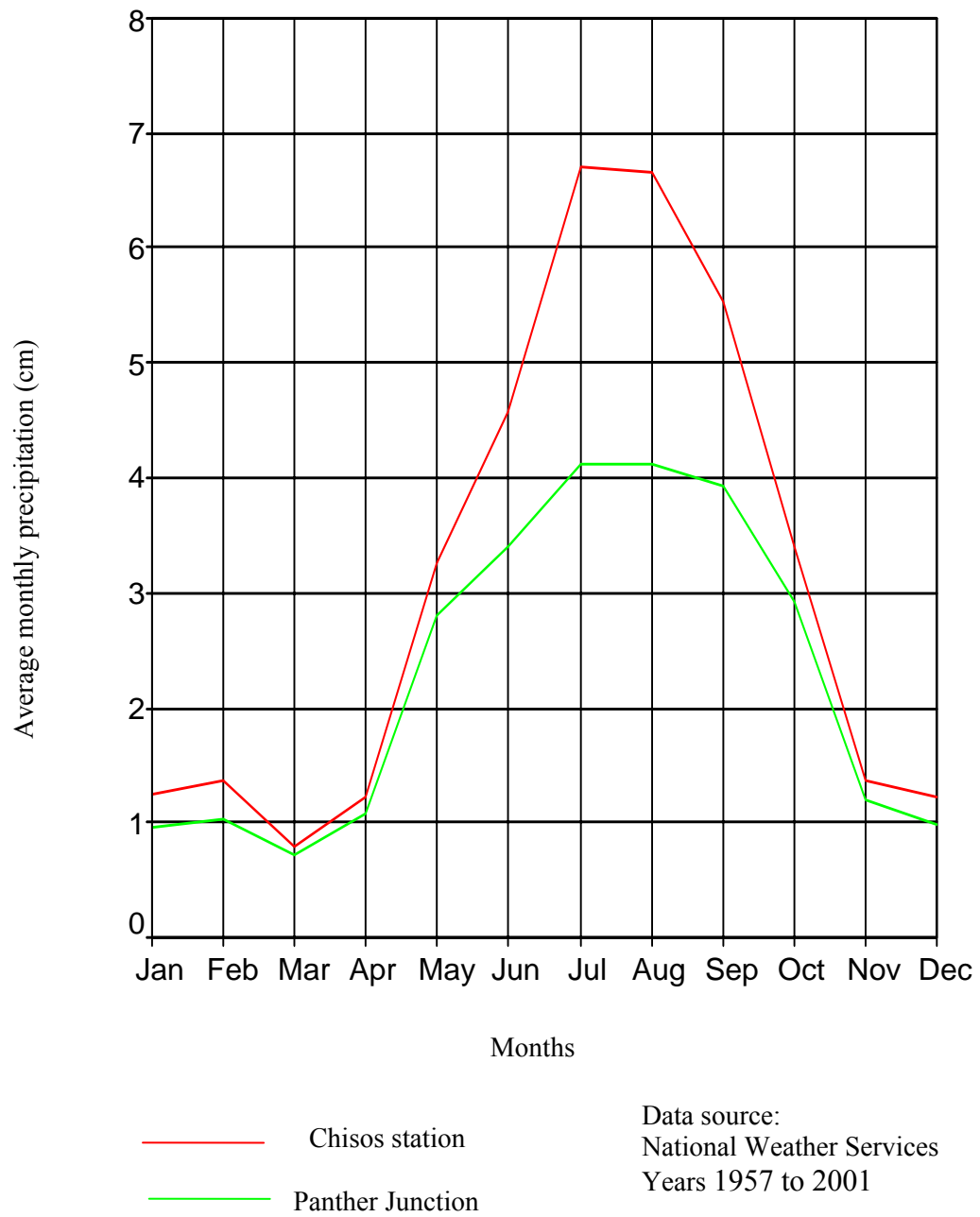


Fig. 4: Average monthly distribution of rainfall over Panther Junction and Chisos Basin, Big Bend National Park, Texas.

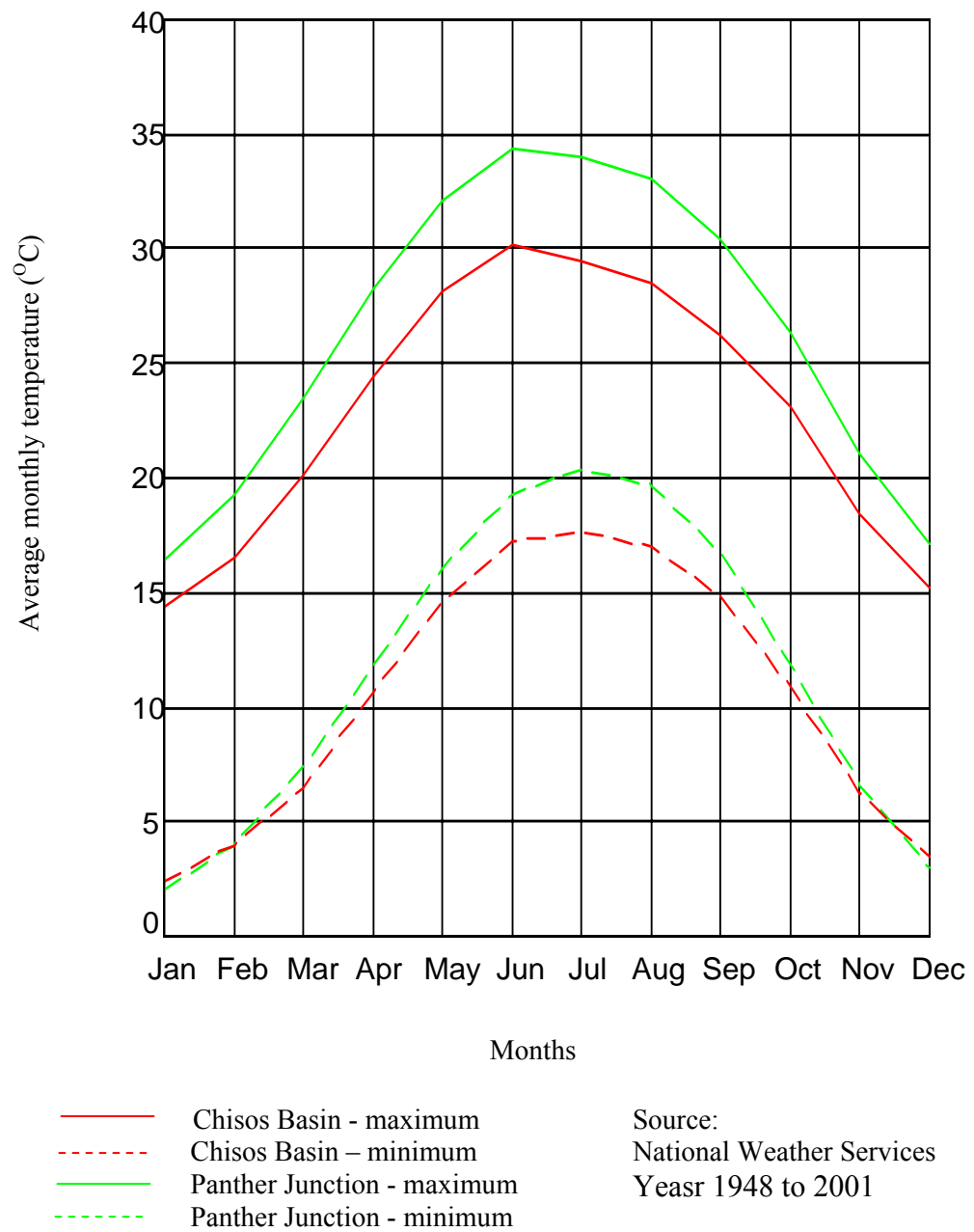


Fig. 5: The distribution of the average monthly temperature over a period extending from 1948 to 2001 at Chisos Basin and Panther Junction climatic stations, Big Bend National Park, Texas.

changes occur in summer months. Diurnal changes affect, markedly, various Earth surface processes such as weathering. Insulation in arid and semiarid landscapes occurs as a result of diurnal variation. Insulation aids in rock disintegration as a result of daily temperature changes (Fig. 7). Rock disintegration by insulation and other weathering processes produces rock debris in winter that can be transported by flash floods in the summer (Goudie 1997). This process reflects the seasonal interaction between geomorphic processes in arid landscapes.

Geology

Rock Types

The study area is characterized by the presence of igneous and sedimentary rocks. Igneous rocks are located in the middle and western part of the study area. Sedimentary rocks occur at the outlet of the drainage basin. The majority of the drainage basin, which is located between sedimentary rocks in the east and the igneous rocks in the west, is covered by surficial deposits (see figure on page 35). The following discussion about the lithologic composition is based on the comprehensive work of Maxwell et al. (1967) on Big Bend National Park.

The igneous rocks include both volcanic and plutonic igneous masses. They represent ~25 % of the study area. The Tertiary volcanic igneous rocks comprise, in an ascending order, the Canoe Formation, the Chisos Formation, and the South Rim Formation. The Canoe Formation occurs in the middle of the study area as a NW-SE

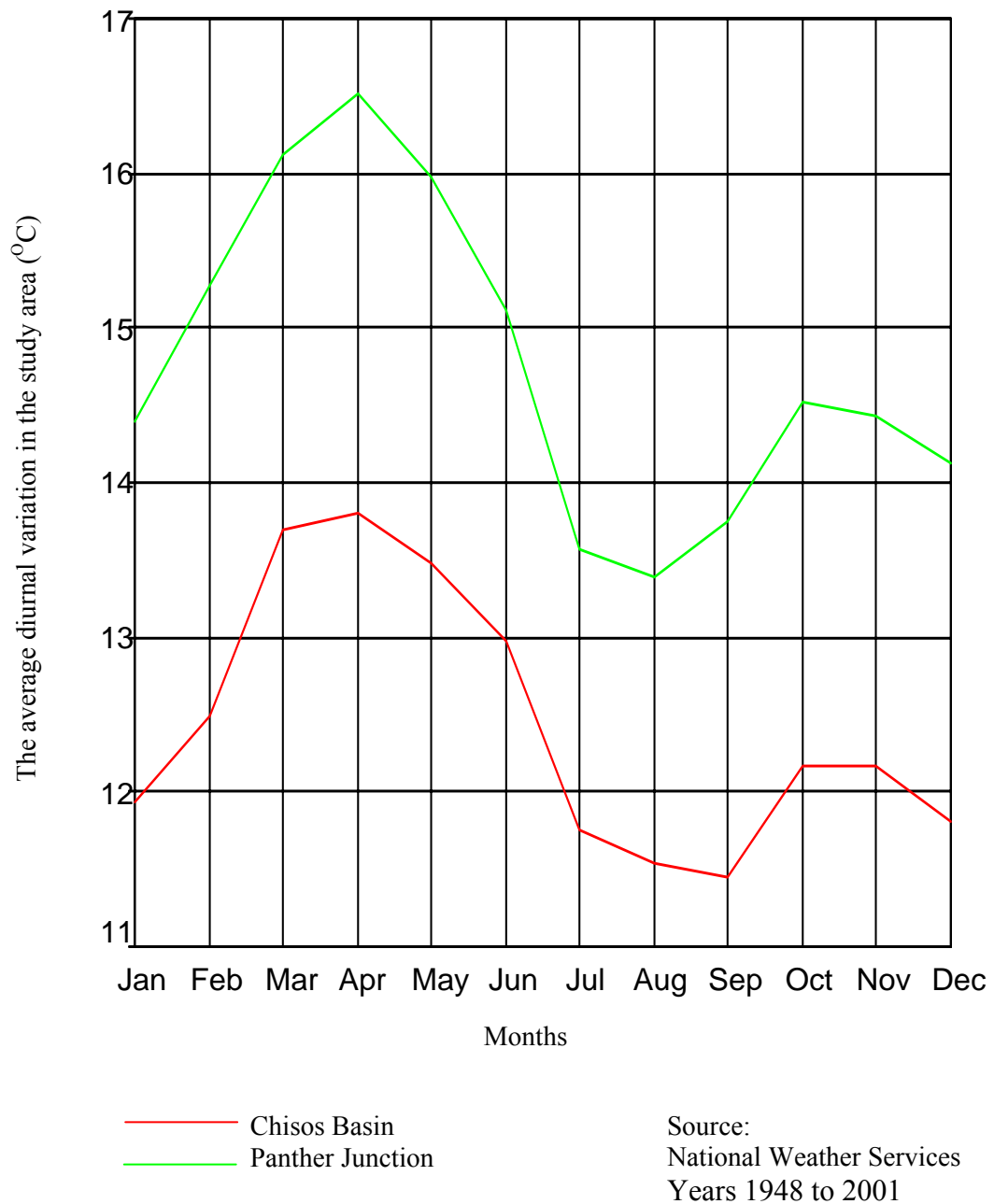


Fig. 6: The diurnal variation at both Chisos Basin and Panther Junction stations, Big Bend National Park, Texas.



Fig. 7: Rock disintegration in the high gravel terrace of the study area (Pen for scale). Photograph taken by author.

wide strip at the foot of the high-level gravel terrace. At the K- Bar Range, a narrow strip of the Canoe Formation occurs along the eastern side of an igneous intrusion. The formation is mainly massive conglomeratic sandstone. The Chisos Formation in the study area is mainly coarse-grained sandstone with beds and lenses of tuffaceous clay, mudstone and massive conglomerate. The South Rim Formation is composed of rhyolite, breccia and rhyolitic lava. The Tertiary igneous rocks range in ages from Middle Eocene for the Canoe Formation, Upper Eocene for the Chisos Formation and Upper Oligocene for the South Rim Formation. In addition to the extrusive volcanic igneous rocks, plutonic igneous rocks occur as scattered masses in the western part of Estufa Canyon drainage basin. They are composed of rhyolite, micorgranite, granophyre, and trachyte.

At the mouth of Estufa Canyon, two formations of the Upper Cretaceous occur: the Pen Formation and the Aguja Formation. Both of these formations occupy a small area of ~5 %. The Pen Formation is composed of clay with scattered sand bodies. The formation is soft and less resistant to erosion. Generally, it forms low topographic areas in the Park. The Aguja Formation is composed of both marine and non-marine deposits. It is a mixture of sandstone, clay, and limestone. Between the outlet of Estufa Canyon at Tornillo Creek Valley in the eastern part of the study area and the igneous rocks in the western part of the study area, an extensive area of surficial deposits occurs (Fig. 8).

The majority of the study area is occupied by surficial deposits (~74 %). It comprises the Holocene unconsolidated alluvial deposits and the consolidated Miocene to Pleistocene deposits. The Holocene alluvial deposits flank the Chisos Mountains to

the east of the study area forming a wide alluvial surface (Fig. 9). The alluvial surface, in turn, is flanked to the east at the middle of the study area by a high level gravel terrace (Fig. 10). Thurwachter (1984) studied the sedimentary facies of the high gravel terrace in detail. He recognized two main members: the lower La Noria Member and the upper Estufa Member (Fig. 8). The La Noria member includes various lithofacies that characterize various depositional environments. In the study area, the La Noria member is represented by sandy facies and the calcrete rich gravel/sand facies. Sandy facies show upward fining and imply deposition in a distal part of a braided stream environment whereas calcrete rich gravel/sand facies represent deposition in a strike-valley developed on the Cretaceous rocks and as small alluvial fans shedding off the Cretaceous slopes (Thurwachter 1984). The sandy facies of the La Noria Member is flanked to the west by the gravel of the Estufa Member.

The gravel lithofacies cover most of the eastern half of the Estufa drainage basin. These lithofacies represent deposition in a proximal alluvial-fan environment. Clast sizes, clast lithofacies, and paleocurrent data show that these alluvial fan deposits were derived from the Chisos Mountains in the west (Thurwachter 1984). To the west of the high terrace level gravels, gravel and silt of Pleistocene and Holocene ages occur. These deposits are derived, mainly, from the adjacent Chisos Mountains.

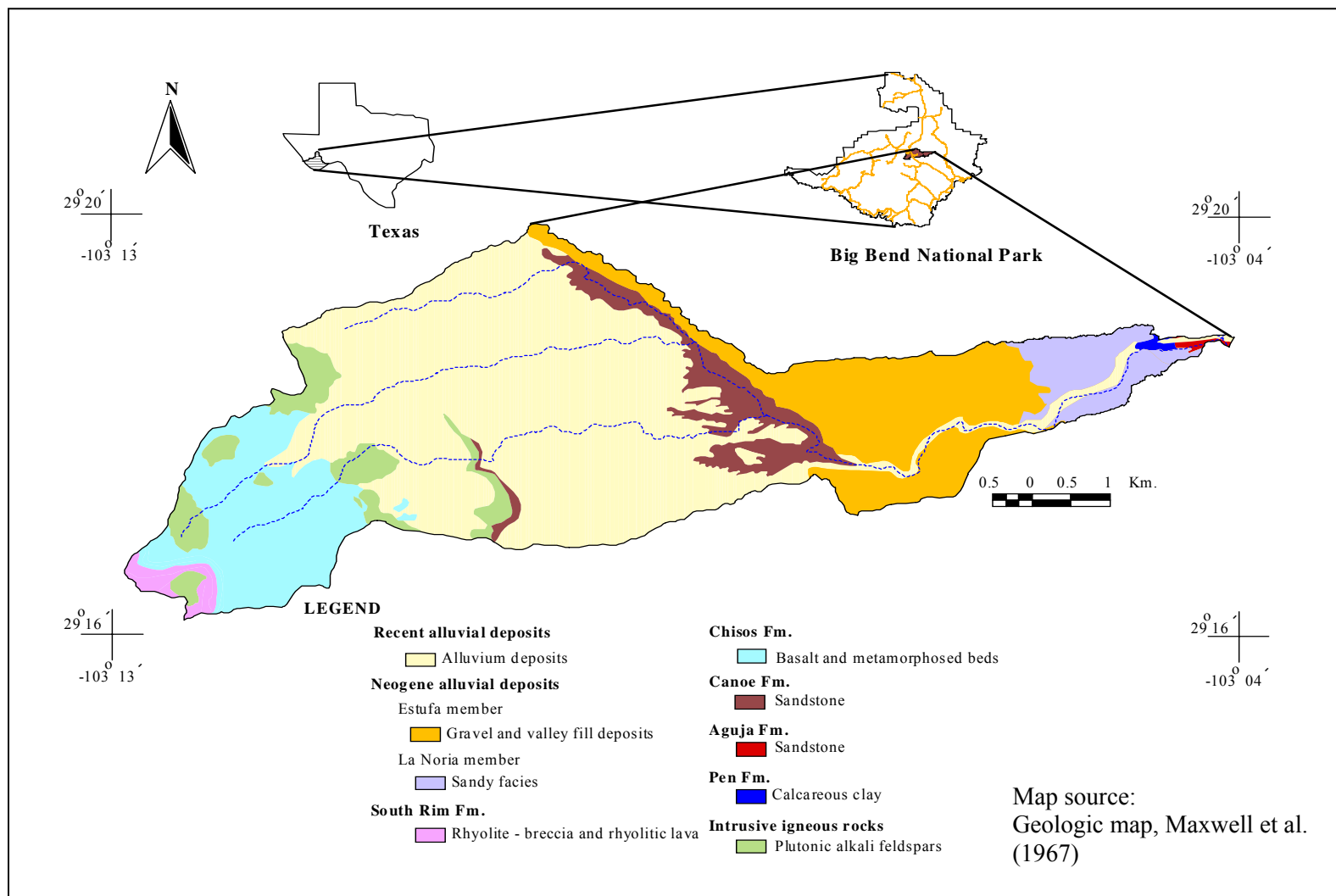


Fig. 8: Geologic map of Estufa Canyon.



A, Holocene unconsolidated alluvial deposits
 B, Canoe Formation at K-Bar Range
 E, South Rim Formation

C, Plutonic igneous rocks
 D, Chisos Formation

Fig. 9: Igneous rocks in the western part of Estufa Canyon and Quaternary unconsolidated deposits. Photograph taken by author.



- A, Unconsolidated Holocene alluvial deposits
- B, Consolidated Neogene surficial deposits
- C, Shrub lands

Fig. 10: Holocene alluvial deposits flanked by a high terrace of Neogene gravel. Photograph taken by author.

Tectonics

In Big Bend National Park, Udden (1907) named and described the Sunken Block, a ~64 km wide Tertiary Basin. The Basin trends northwest and is bounded by the Santiago Mountains and Sierra del Carmen along the east of the Park and by Mesa de Anguila and Solitario Dome on the western edge of the Park. In the center of the Sunken Block, are the Chisos Mountains. This regional tectonic setting is the result of Laramide Orogeny and Basin and Range deformations.

The Laramide Orogeny is a compressional tectonic event that began in the Late Cretaceous (70 Ma) and ended during the middle Eocene (50 Ma). The Laramide Orogeny resulted in structural features trending NW and E-W directions (Dickerson 1980). These structural elements include folding and thrust faulting (Muehlberger 1980). Sierra del Carmen, a west dipping monocline of Cretaceous rocks (Maxwell et al. 1967), and Tornillo Basin, a Laramide-age sedimentary basin in the Trans-Pecos region of West Texas (Lehman 1991) were produced during the Laramide Orogeny. A transition period from the dominant compressional stress of Laramide Orogeny to the dominant tensional stress of Basin and Range deformation has been defined by Wilson (1959) and Stevens and Stevens (1985). This transition period started in Late Eocene and extended nearly through the Oligocene (Wilson 1959). During the transition period, volcanic activities occurred producing the Chisos Mountains, which form the geographic center of the Sunken Block. A shift from the mixed compressional and tensional stresses (the transition period) to dominant tensional stress occurred ~ 26 – 25 Mya or younger (Stevens and Stevens 1985). The tensional deformation resulted in an episode of Basin

and Range extensional faulting. Northwest-oriented normal faults cut both the Sunken Block and the monocline of Sierra del Carmen producing horsts and grabens. These tectonic events affect directly the topographic variations in the study area.

To the west of the study area, George Wright Peak and Pummel Peak of the Chisos Mountains occur. These peaks are flanked eastward by igneous intrusion masses that are flanked to the east by a wide basin formed by older tectonic events (Fig. 9). Close to the igneous intrusion, other N-S trending igneous intrusion masses occur around the K-Bar Range area. These masses occur around a NW-SE trending anticline called Lone Mountain anticline. At the eastern boundary of the alluvial surface, a NW-SE abrupt elevational increase (Fig. 10) occurs as a result of Quaternary tectonic (Maxwell et al. 1967 and Steven and Steven 1985). These tectonic settings along with the lithologic composition affect the topography and landforms of the geomorphic systems in the study area.

Soil

Climate and the composition of the bedrock control the weathering rates and the erosional products that compose the soil in the study area. Soil plays an important role in controlling mass movement in the landscape. In combination with the slope and moisture content, soil texture controls the types of mass movement that occur in geomorphic systems. In the study area, soil varies spatially. There are five main soil classes (Fig. 11). These classes include Brewster – Rock outcrop complex, Lajitas – Rock outcrop complex, Chilicotal – Monterosa association, Chamberian gravelly loam, and Chilicotal

gravelly fine sand loam complex (United States Department of Agriculture 1985). The Brewster – Rock outcrop complex occurs in the steep, hilly area of Chisos Mountain in the west of the study area. This class consists of a layer of reddish very cobble loam. The Brewster – Rock outcrop complex is flanked eastward by the Lajitas outcrop complex that is a hilly terrain. The Lajitas complex is composed of cobbly loam resting abruptly on hard igneous rocks. The Chilicotal – Monterosa association class occurs as a rolling. The Chilicotal – Monterosa association is composed of gravelly fine sandy loam. It flanks igneous masses in the western part of the study area and cover the gravelly dominated area of the high gravel terrace in the middle of the study area. The last two soil classes are characterized by finer grain sizes. The Chamberian gravelly loam occurs in the eastern part of the study area whereas the Chilicotal gravelly fine sand loam soil class occupies the alluvial surface of the study area. Each soil class has its own soil texture and composition characteristics. The textural variations of soil in the study area reflect high variations in the surface roughness over various landforms that form the Estufa Canyon.

Vegetation

Big Bend National Park is an example of the Chihuahuan Desert arid climate (Plumb 1992). Plumb (1992) grouped the vegetation cover types of Big Bend National Park into four sub-environmental regions. These regions are riparian; desert plains and badlands; desert mountains, foothills and mesas; and high Chisos Mountains. In the study area, each sub-environmental region is characterized by associations of vegetation

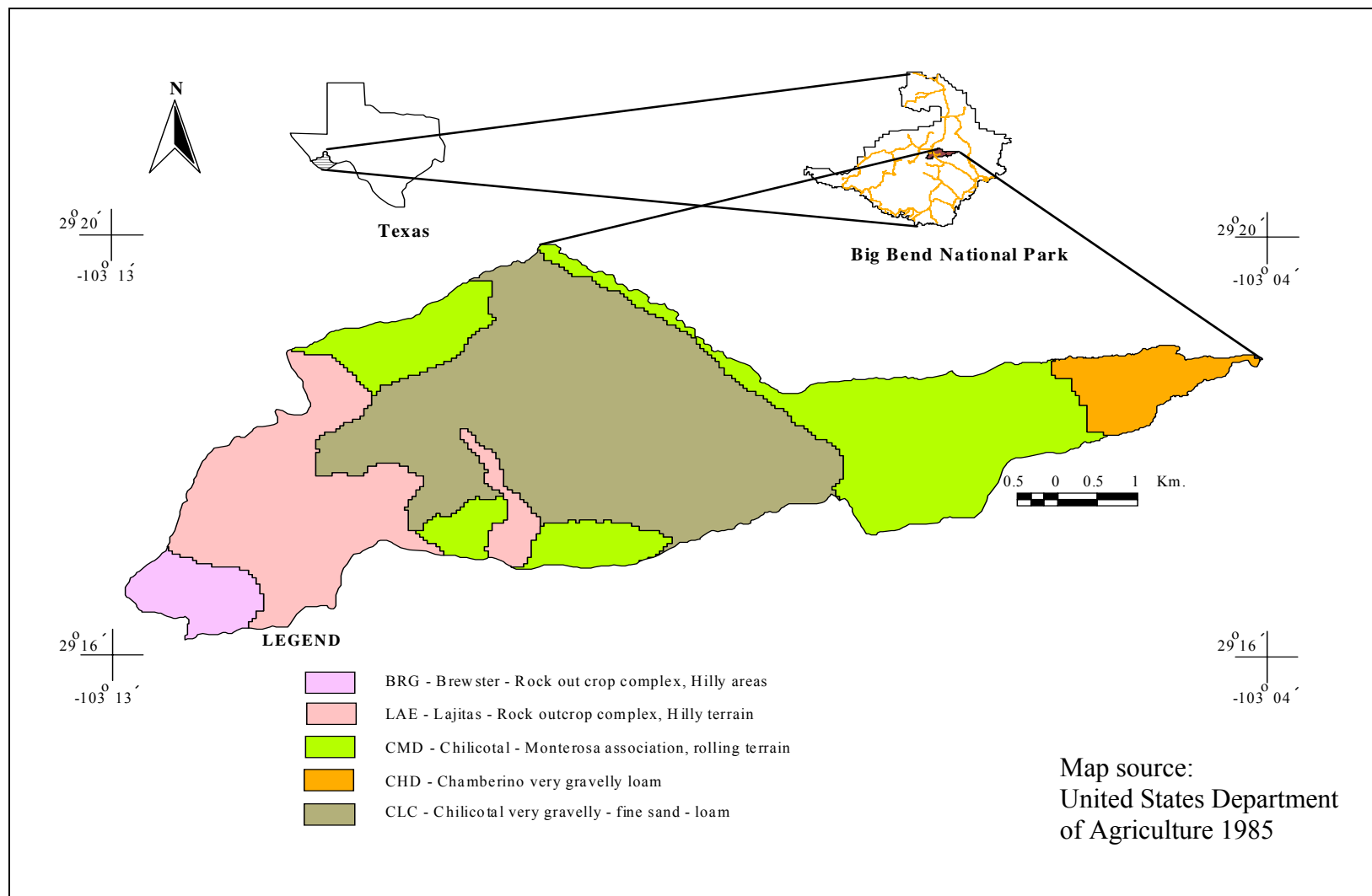


Fig. 11: Soil map of Estufa Canyon.

cover types (Fig. 12). Creosote – Lechuguilla, Creosote – Grass, and Creosote – Turbush cover types are dominant in the desert plains sub-environmental region. These cover types represent the shrublands in the middle of the study area. The majority of the study area is occupied by various grassland cover types such as Lechuguilla–Grass – Viguiera, Lechuguilla–Grass, Sotol–Lechuguilla–Grass, and Sotol–Nolina–Grass. These vegetation cover types occur in another sub-environmental region that includes the desert mountains and the foothills. The first two cover types of this environmental region occur in the low elevations whereas the last two cover types occur in the high elevations. At the high elevations of the Chisos Mountains sub-environmental regions, woodlands occur. The Pine–Juniper–Grass vegetation cover mainly represents the woodland areas. Generally, vegetation cover is a sensitive indicator for environmental change. The change of vegetation cover as a response to climatic change influences, accordingly, the types and intensity of various geomorphic systems.

Grasslands are sensitive to environmental change even over short temporal scales (Ludwig et al. 2000). This sensitivity resulted in the replacement of grasslands into shrublands in considerable areas of Big Bend National Park (Wondzell and Ludwig 1995 and Purchase 2002). The change from grasslands to shrublands increases the rates of surface runoff and soil erosion (Schlesinger et al. 1999). Increasing surface runoff and soil erosion enhance degradation processes in some places where rills and gullies evolve. In other places, aggradation processes increase resulting different landforms such as alluvial fans (Parsons et al. 1992).

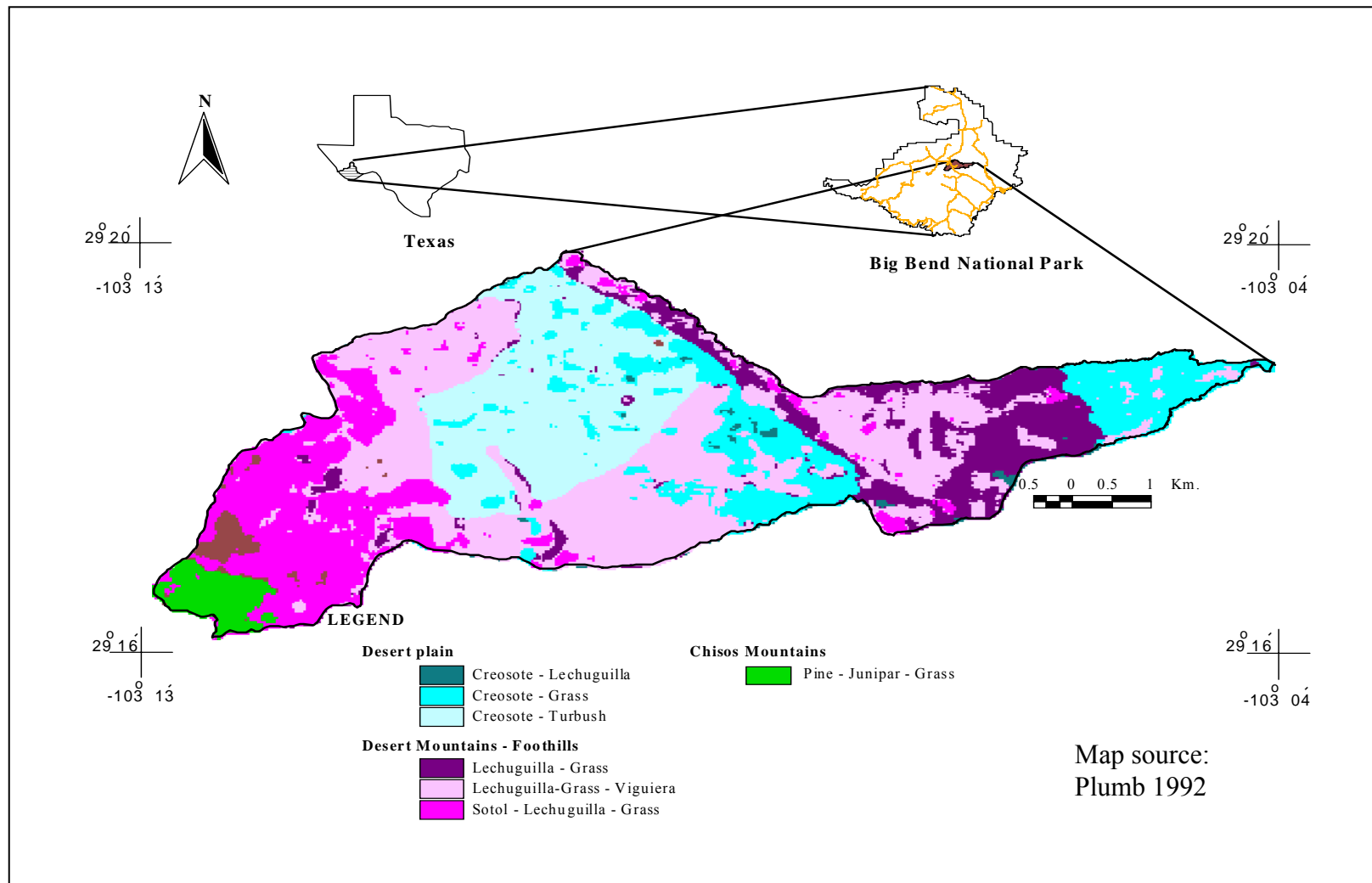


Fig. 12: Vegetation cover of Estufa Canyon.

The aggradational and degradational processes affect the overall connectivity between geomorphic systems of the landscape.

Geomorphology

The study area is composed of two terrains: the western terrain and the eastern terrain. Both terrains are separated by the N-S trending section of the Estufa main channel. The western terrain is composed of the mountainous area and the alluvial deposits whereas the eastern terrain can be subdivided, composition wise, into gravel dominant area in the middle of the study area and the sandstone dominant area in the eastern part of the study area. The geomorphic systems of each terrain are connected by various spatial links. The main trunk channel of Estufa Canyon is the main interconnecting spatial link between the geomorphic systems of the western and the eastern terrains. Reviewing the topographic and compositional settings of each terrain will help understand the connectivity between various geomorphic systems in the study area.

The Western Terrain

The mountainous area of the western terrain is composed of igneous rocks of various compositions and elevations. Under the arid climatic region and the sparse vegetation cover, differential weathering results in rock disintegration producing rock fragments of various sizes. Transporting the weathering product within and from the mountainous area is controlled by the topographic setting. The domal mountain area is

characterized by high values and spatial variabilities of elevation and slope. The elevation of the domal mountain area ranges from 1,094 to 1,975 m with a mean of 1,346 m. The relief of this terrain is 881 m over a maximum horizontal distance of ~ 4 km. Along this distance, the slope is highly varied. Slope values vary from 0.33° to 54.0° with a mean of $\sim 16.11^\circ$ and standard deviation of 9.56° . The main slope surface in the domal mountain area ranges from strongly inclined ($5.00 - 15.0^\circ$), steep ($15.0 - 25.0^\circ$), very steep ($25.0 - 35.0^\circ$), to precipitous ($35.0 - 90.0^\circ$). The high relief and steep slopes of the mountain area provide gravitational forces required for mass movement in the geomorphic systems of this area. The mountain terrain is dissected by straight, steep, and deep stream channels. These channels are responsible for transporting the debris from the mountain area to the alluvial deposits.

The alluvial deposits are located between the mountain terrain in the western part of the study area and the high-level gravel terrace in the east. These alluvial deposits represent a transitional surface between the mountain terrain and the high-level gravel terrace terrain. The area of the alluvial deposits is a broad surface with a gradient ranging from 0° to $\sim 23^\circ$ with an average gradient of 2.5° . The average slope value indicates a gently inclined surface. The surface of the alluvial deposits is dissected by parallel eastward trending channels (Fig. 13). These channels transport the mass from the area of the alluvial deposits to the main N-S trending trunk channel of Estufa Canyon. The connectivity potential of these channel systems to transport mass depends on whether the geomorphic process is erosional or depositional in the area of the alluvial deposits.

The N-S trending trunk channel represents the essential spatial link that connects the western terrain to the eastern terrain. The N-S trending trunk channel extends from the central north boundary of the study area to the central south boundary of Estufa drainage basin. The N-S trending trunk channel bends at the central south boundary eastward to Tornillo Creek. The channel is straight, narrow and deep. The elevation of this channel ranges from 920 m to 975 m with a total relief of 55m. The slope of the channel varies from 0° to 6.5° m with a mean slope of $\sim 2^{\circ}$. This channel segment represents the main connecting spatial feature between the area of the alluvial deposits and the high-level gravel terrace area in the eastern terrain.

The Eastern Terrain

Based on the lithologic composition, the eastern terrain can be subdivided into two areas. The gravel dominant area in the middle of the study area and the sandstone dominant area in the eastern part of the study area. Both of the areas are different in spatial distribution, topography, and landforms. The gravel dominant area occurs in the middle of the study area whereas the sandstone dominant area occurs east of Estufa drainage basin. The elevation of the gravel area ranges from 816 m to 1,049 m with a mean of 930 m. The slope of this terrain varies from 0° to $\sim 30^{\circ}$ with an average of $\sim 6^{\circ}$ reflecting a strongly inclined surface. This terrain is mainly composed of isolated drainage basins and hillslopes. The drainage basins of this area drain either directly to the main trunk channel of Estufa Canyon or pass through the main stream channel in the sandstone area (Fig. 13). The surface of the drainage basin in this terrain is composed of

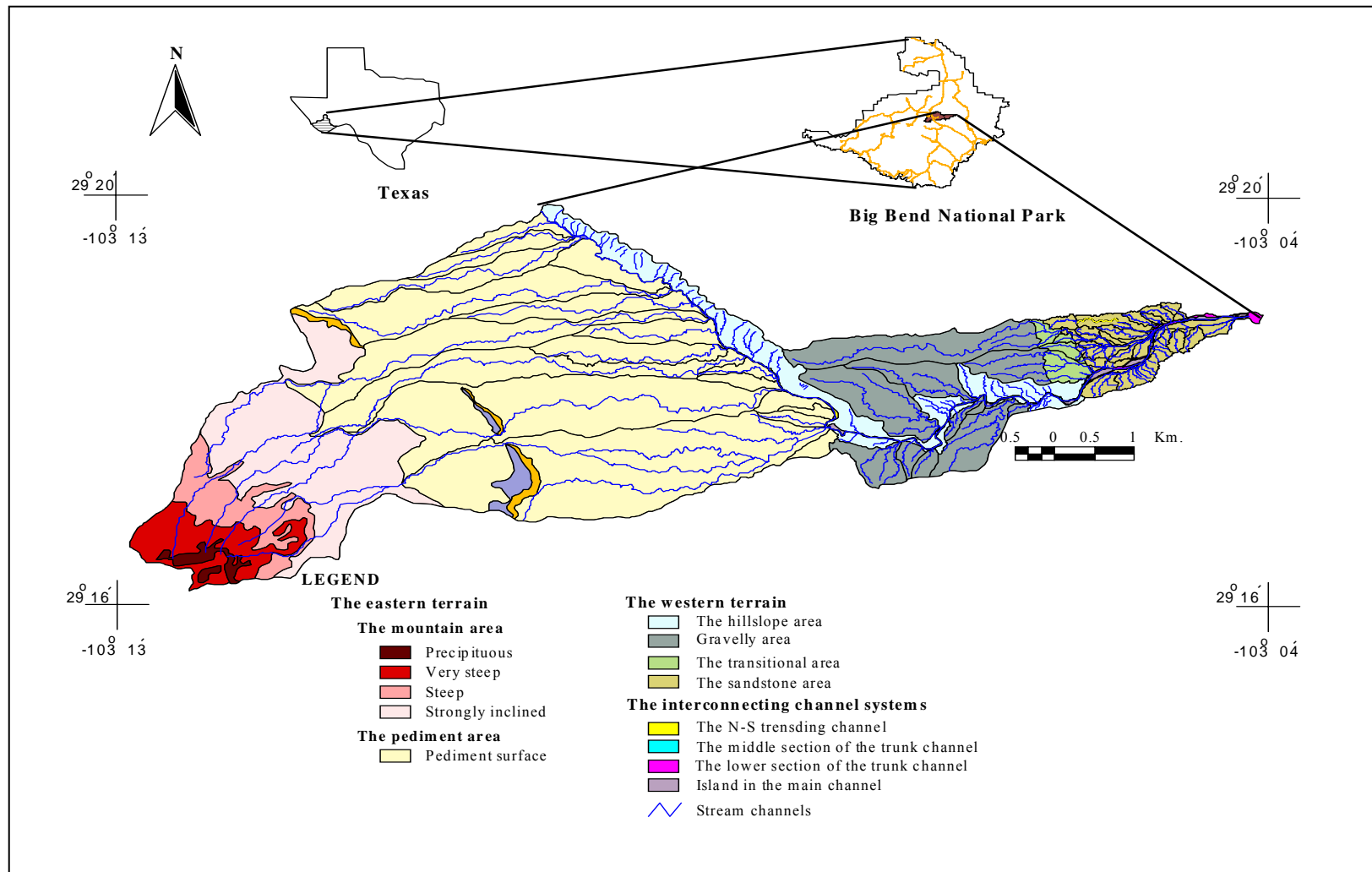


Fig. 13: The main geomorphic units of Estufa Canyon.

gravelly broad elongated hills with a coarse drainage density. The hillslopes of the gravel area drain directly to the main trunk channel. The main trunk channel that connects the drainage basins and the hillslopes of the gravel area extends from the N – S trending trunk channel to the eastern boundary of the gravel area. The N-S trending trunk channel drains the east sloping hillslopes of the eastern terrain. The south and the north trending drainage basins and hillslopes are connected by the middle range of the main trunk channel in Estufa Canyon. This section of the trunk channel extends from the outlet of the N-S trending section eastward to the boundary of the gravel area. This middle section of Estufa Canyon is a dynamic section.

The elevation of this section ranges from 815 m to 917 m with a relief of 102 m over an overall distance of 3.3 km. The slope ranges from 0.95° to $\sim 27^\circ$ with an average of $\sim 8^\circ$ reflecting a strongly inclined surface. This section has steep walls and a narrow cross-section. At the end of the gravel area, the width of the main trunk channel remarkably increases with the presence of wide in-channel islands.

To the east of the gravel area, the sandstone area occurs. The sandstone area has elevations that range from 734 m to 865 m with a mean of ~ 800 m and relief of 131m. The slopes in this terrain range from 0° to $\sim 26^\circ$ with an average of $\sim 5^\circ$ reflecting a gently inclined surface. The sandstone area is highly dissected by short stream networks that form small drainage basins. These drainage basins drain directly to the mainstream channel. Alluvial plains are limited or almost absent in the sandstone areas. Some main channels north of the main trunk channel connect the geomorphic systems of the

gravelly sub-terrain to the sandstone area. The downstream section of the main trunk of Estufa Canyon passes through the sandstone area to Tornillo Creek in the east.

The elevation of the lower section of the main trunk channel in the Estufa canyon ranges from 727 m to 819 m with a relief of 92 m along a maximum distance of 2.3 km. The slope ranges from 0.34° to 13.2° with an average of 3.71° reflecting a gently inclined surface.

The climatic, geology, soil, and vegetation, along with the geomorphic characteristics, affect the spatial variability of the potential of the geomorphic systems for transporting mass in the study area. Under arid conditions where the rates of evaporation exceed the rates of precipitation, mechanical and biochemical weathering processes disintegrate the bedrock into fragments of various sizes. The high variabilities of rock resistance to weathering agents result in enhancing differential weathering producing various slopes in the study area. Over these slope, soils of various grain sizes are deposited. During summer, flash floods take place. A large amount of debris is transported by deep and narrow streams in eastward directions from the high elevations in the western part of the study area with high kinetic energy. The velocity of the stream channels decreases at the mountain front of the source rocks resulting in the deposition of the debris in the area of the alluvial deposits. The coarser debris is deposited close to the mountain front whereas the finer debris is transported by deep narrow streams that incise the surface of the alluvial deposits. The dominant geomorphic processes, i.e., erosional or depositional, in the area of the alluvial deposits is not only controlled by the high kinetic energy of the stream channels that transport mass in the downstream

direction from the source rocks to the area of the alluvial deposits but also on the change of landscape gradient of the geomorphic systems that flank the area of the alluvial deposits in the downstream direction. The change in the landscape gradient either maximizes or minimizes the mass transportation in the area of the alluvial deposits. An increase of the slope gradient results in maximizing mass transportation in the area of the alluvial deposits whereas a decrease in the landscape gradient results in minimizing the mass transportation in the area of the alluvial deposits. Maximizing or minimizing mass transportation in the alluvial deposits accordingly affects the rates and intensity of the erosional processes in the high elevations in the western part of the study area. Maximizing mass transportation implies the presence of a high connectivity potential between various geomorphic systems in the fluvial systems, whereas minimizing mass transportation imply low connectivity potential between various geomorphic systems in the fluvial systems.

To study these complex relationships at the scale of the fluvial system, a methodology was established to determine an index of the connectivity potential for the geomorphic systems that form the fluvial system. The index facilitates the understanding of the mutual relationships between various geomorphic systems. These relationships can be used to define the system-wide connectivity in the fluvial system. The landscape gradient and the surface roughness were integrated to determine the index of the connectivity potential between the geomorphic systems. The index represents a surrogate that expresses the potential of the geomorphic system for transporting mass in the landscape.

CHAPTER IV

DATA DESCRIPTION AND STUDY METHODOLOGY

Introduction

Two main types of data were used to accomplish the objectives of this study: topographic data and satellite imagery. The topographic data are represented by the Digital Elevation Model (DEM) whereas the satellite imagery is represented by the Digital Orthophoto Quadrangles (DOQ) and a Radarsat-1 image. Various thematic layers were extracted from the DEM and the satellite images. These thematic layers include slope, the trunk stream, and geomorphic systems. The Radarsat-1 image was digitally processed to produce a backscattering coefficient image that represents the surface roughness of the study area. The raster slope layer and the backscattering image were combined together to produce an image that represents the connectivity potential index in the study area. The index image was used to extract the mean index of various geomorphic systems in the study area using various GIS operations. The mean index of each geomorphic system represents a surrogate of the connectivity potential of the geomorphic system. A system-wide connectivity of the fluvial system of the study area has been evaluated by determining the ratios between the connectivity potential index of the upstream geomorphic systems and the connectivity potential of the downstream geomorphic system. A methodology was developed to perform these objectives. A flow chart showing the main steps of performing the methodology is illustrated in Fig. 14.

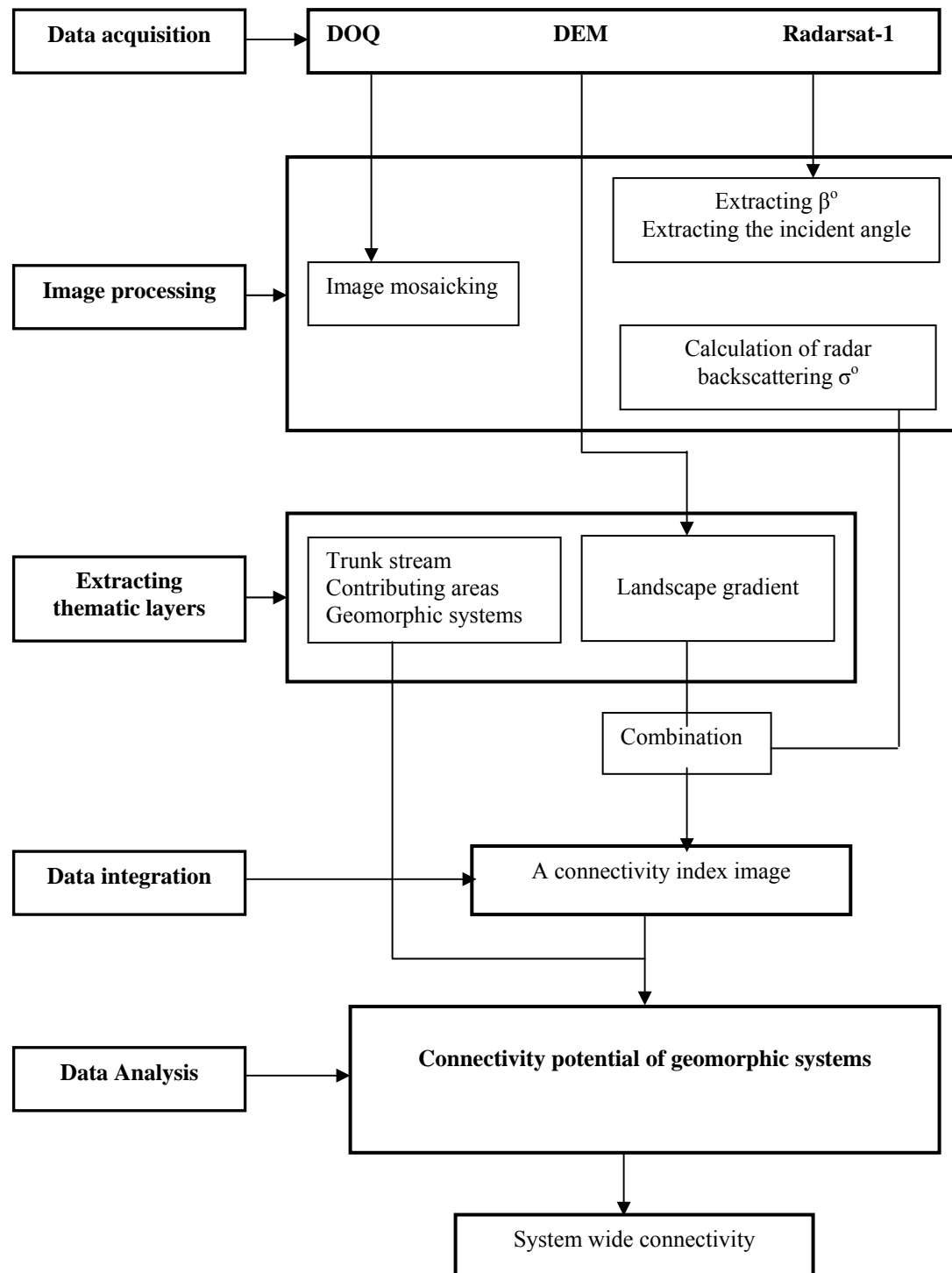


Fig. 14: A flow chart showing the methodology of studying the connectivity potential of geomorphic systems.

Data Acquisition and Description

Digital Elevation Model

The digital elevation model is a grid representation of surface elevations. Each grid cell is characterized by an x, y location. Every cell has a z value which is the elevation of that location. The spacing between each grid cell is the spatial resolution of the DEM. A Digital Elevation Model of 30-meter spatial resolution that covers the study area was obtained from the Texas Natural Resources Information Systems, (TNRIS), (Table 1).

Digital Orthophotos Quadrangle (DOQ)

A set of color-infrared digital orthophoto images that cover the study area were acquired from the Texas Natural Resources Information Systems, (TNRIS). The study area is located in an area that is covered by various portions of six contiguous digital orthophoto images. These images are the northwest image of the Panther Junction quadrangle, the southwest image of the Panther Junction quadrangle, the Northwest image of the Roy quadrangle, the southwest image of the Roy quadrangle, the northeast image of the Roy quadrangle, and the southeast image of the Roy quadrangle. The digital orthophoto images that were obtained from the TNRIS are scanned aerial photographs that have been derived from the 1: 40,000 NAPP (National Aerial Photography Program) photography taken in the 1994 – 1997 period. These photographs were digitally corrected to remove distortions that are produced from the camera, tilt and ground relief. The spatial resolution of the digital orthophoto images is 1-meter. With

this fine resolution, it is possible to map spatial features such as the boundaries between various geomorphic systems of the study area that were screen digitized. Data specifications of the digital orthophoto images are shown in Table 1.

Radarsat Image

A radar image acquired by the Canadian Radarsat-1 satellite on January 2003 was used to study the surface roughness of the study area. The Radarsat-1 satellite acquires images using its own source of energy. It transmits energy at the wavelength 5.60 cm which is known as “C” band. The transmitted energy “illuminates” the surface of Earth using sideways – looking direction geometry (Drury 2001). The illumination process occurs by transmitting radar microwave pulses. The pulses "sweep" the land from the near range to the far range across the radar swath area (Fig. 15). The transmitted radiation is horizontally polarized. Only, the horizontal component of the returned radar backscatter is received by the antenna. The Radarsat-1 satellite acquires various beam modes at various spatial resolutions. In each beam mode, various beam positions are acquired as well at various incident angles. The beam mode of the radar image that covers the study area has a spatial resolution of 6.25 m with a beam position of average incident angle of 43.11° . The smaller the spatial resolution, the higher the details the Radarsat-1 image provides. As the incident angles increase, more detail about the surface roughness is provided. The Radarsat-1 satellite acquires radar imagery also in two different directions: a west looking direction that is known as descending look

Table 1

Data Specifications of various data used for analysis

Specifications	DEM	DOQ	Radar imagery
Scale	Digital	Digital	Digital
Source	TNRIS, Texas	TNRIS, Texas	Radarsat international, Canada
Spatial resolution	30 meters	1 meters	6.25 meters
Data type	Digital elevation	Digital optical data	SGF data product – ground range data
Wavelength	--	Color infrared	C band
Polarization	--	--	HH
Beam mode	--	--	Fine beam
Incident angle	--	--	43.11°
Look direction	--	--	West looking – descending
Projection	UTM	UTM	Georeferenced
Data extracted	Slope	Base map	Brightness image
	Aspect	Geomorphic systems	Incident angle image
	Downslope index	Stream network	Backscatter image
Software used for data processing	ARCVIEW®	ERDAS IMAGINE®	PCI®

- UTM, Universal Transverse Mercator
- PCI, A digital image processing software

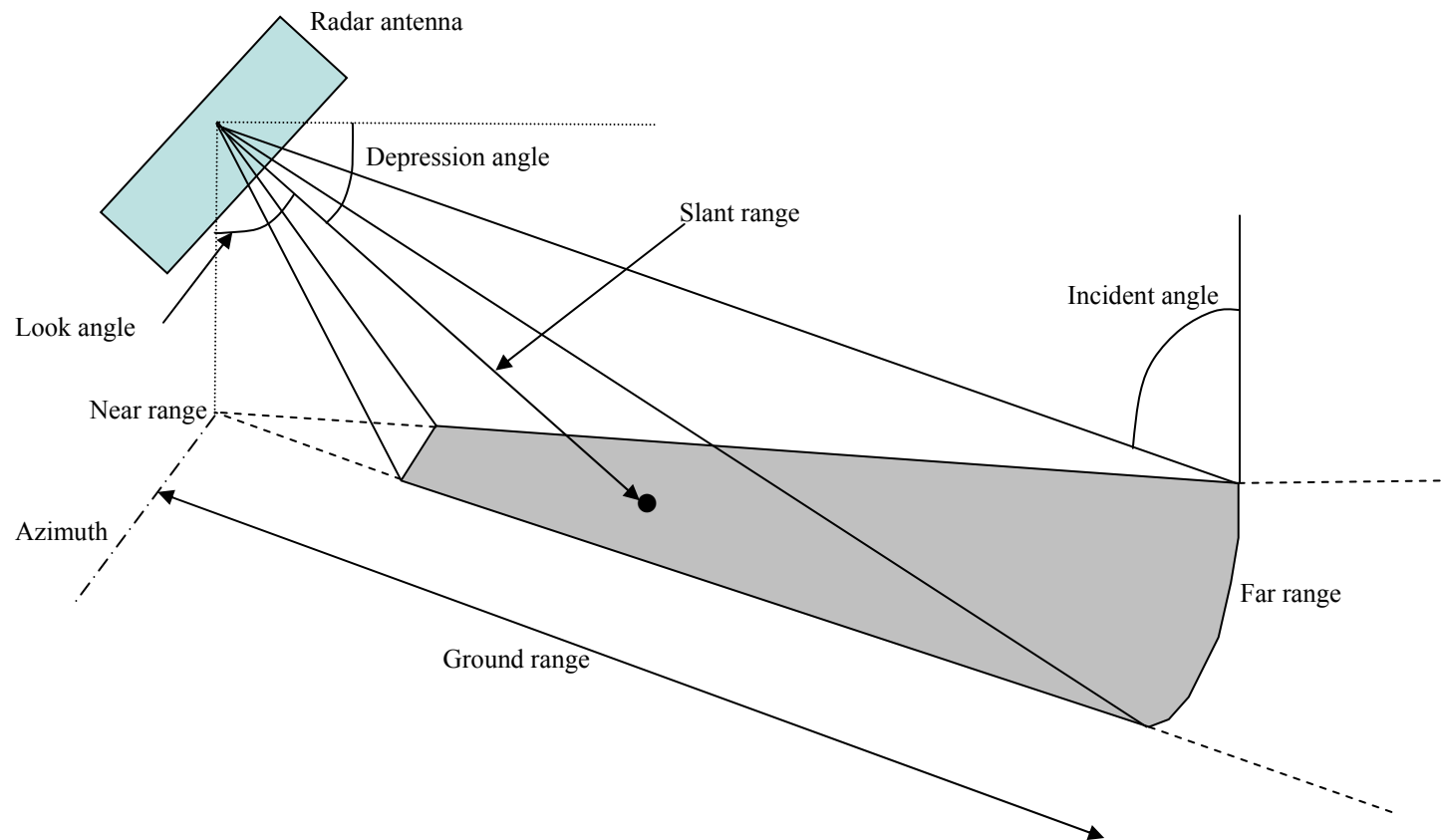


Fig. 15: A drawing shows the geometry involved in a sideways-looking radar-imaging system. The depression angle is the angle between horizontal and a radar ray path. The look angle is the angle between vertical and array path. The incident angle is the angle between an incident radar ray and a line at right angles to the surface, modified after Drury 2001.

direction and an east looking direction that is known as ascending look direction. The image that covers the study area is acquired by a west looking (i.e., descending) antenna. After acquiring the radar images, these images pass through various digitally enhancing processes to produce various products. The SGF (Sar Georeferenced Fine resolution) path image product is one product that can be used to calculate the radar backscattering coefficient from the radar image.

The SGF product of the Radarsat-1 satellite was used to calculate the radar backscatter of the surface of the study area. The product is a path product where the image is oriented in the satellite direction. It is informative to note that it has all the required information in its header files to calculate the radar backscatter using commercial software. A full description of the product is available in Table 1.

An objective interpretation of radar images depends basically on an understanding of both the terrain parameters and the radar imaging system parameters. The terrain parameters include slope angle, surface roughness, and dielectric properties. Whereas the radar imaging parameters include wavelength frequency, polarization, look angle, look direction and resolution (Lewis 1998).

Digital Image Processing

Mosaicking the Digital Orthophoto Images

The study area is located in an area that is common between six contiguous digital orthophoto images. This required that the six images be mosaicked. The mosaicking process was carried out via various steps. First, all histograms of the images

were matched using the histogram matching operation of the ERDAS[®] Imagine software. Then the mosaicking operation was applied to the six images to form the final mosaicked image. Image enhancement techniques such as histogram stretching were used to match the boundaries between the mosaicked images. An image covering the study area was subsetting from the mosaicked image.

Extracting Radar Backscattering Coefficient

The intensity of the radar backscatter from a point target is its radar cross-section (Ulaby et al. 1982 and Drury 2001). A measure of the energy backscatter from a target with a large area (i.e., extended target) is the radar backscattering coefficient σ^0 . The radar backscatter coefficient is defined as the average radar cross section per unit area (Ulaby et al. 1982). The radar backscatter coefficient is a fundamental measure of the radar properties of a surface (Drury 2001).

The SGF (Sar Georeferenced Fine resolution) Radarsat-1 product is a path image that has the returned radar signals recorded in the ground range. Like all Radarsat-1 data products, the SGF data product is geometrically and radiometrically calibrated. The product is scaled using a 16-bit dynamic range. The scaling process produces gain offset and scaling data. These data along with the orbit characteristics and the incident angles are required to calculate the radar backscattering coefficient. The calculations of the radar backscattering coefficient were carried out using various modules of the PCI digital image processing software. The process of extracting the radar backscatter coefficient from the SGF data product using PCI software is based on the algorithms

developed by Shepherd (1997). Extracting the radar backscatter coefficient includes the following steps:

- ***Extracting Beta Nought (β^0) from the SGF Data Product***

The gain offset and scaling data of the SGF data product are used to extract the calibrated DN values of the SGF data product in terms of radar brightness (β^0). The radar brightness can be calculated using the SARBETA[®] modules available in PCI[®] digital image processing software. The module uses the following algorithm to calculate the radar brightness:

$$\beta^{0ij} = 10.00 * \log_{10} [(DN * DN + A0)/A_j] \quad (7)$$

where,

β^{0ij} is the output radar brightness of scanline i and a pixel j,

DN is the input image value for scanline i, and pixel j,

A0 is the gain offset, and

A_j is the expanded gain scaling table value for column j.

- ***Extracting the Incident Angle(I_i) for Each Pixel in the SGF Data Product***

Every Radarsat-1 image is acquired at a beam position. A beam position expresses a range of incident angles extending from the near range under the satellite to the far range away from the satellite. To fix the variation in the radar signals as a result of the effect of the incident angles, the incident angles along the ground range

should be determined first. Then, these angles are used to calculate the backscatter coefficients across the ground range.

To calculate the incident angles for each pixel of the SGF data product, three parameters should be determined and calculated first. These parameters are the Earth's radius (r), the satellite altitude (h), and the slant range for each ground range increment of the output scaling look up table (RS_j). These parameters are used by the SARINCD[®] module of the PCI[®] digital image processing software to calculate the incident angle for each pixel using the following algorithm:

$$I_i = \arccos [(h^2 - RS_i^2 + 2*r*h)/(2*RS_i*r)] * 180/PI \quad (8)$$

where,

- I_i is the incident angle at a given column,
- \arccos is the arccosine function,
- h is the orbit altitude in meters,
- RS_i is the slant range at a given image column, in meters,
- r is the radius of the earth at the image center, and
- $180/PI$ is to convert radians to degrees.

- ***Extracting the Sigma Nought (σ^0 , radar backscatter coefficient)***

The radar backscattering coefficient is a measure of various physical characteristics of Earth's surface such as surface roughness and the soil moisture. The surface roughness is a function of the vegetation and grain size variations of the

surface. During times of low moisture content and in an area of scarce vegetation, the backscatter is used to express the granular variations of surface. The radar backscattering then represents the surface roughness that expresses the textural variations of the Earth's surface. Both the radar brightness (β_{ij}^o) and the incident angle I_j , are used by the SARSGM module of the PCI[®] to calculate the radar backscatter coefficient (σ^o) using the following algorithm:

$$\sigma_j^o = \beta_{ij}^o + 10.00 * \log_{10} (\sin I_j) \quad (9)$$

where,

σ_j^o is the radar backscattering coefficient,

β_{ij}^o is the radar brightness, and

$\sin I_j$ is the incident angle.

Speckle Reduction

Speckle noise occurs in remote sensing imagery that is acquired using a coherent radiation in the imaging system such as SAR (Synthetic Aperture Radar) images (Kaun et al. 1987 and Fukuda and Hirosawa 1998). It occurs as a result of the interference of the radar returned signals from each pixel (Goodman 1976). The interference may be a constructive interference producing white pixels or a destructive interference producing black pixels (Fig. 16). Gray shades occur between the white and the black pixels reflecting the mixture component of each pixel in the SAR image. This interference character is attributed basically to the fact that the backscatters of each resolution cell or

pixel is the combined effect of all the objects within the cell that return the radar signal (Lewis 1998). Thus, obtaining meaningful information from the radar images, first, requires removing the speckle noise from the SAR images using various filters.

Various filters are used to remove speckles from SAR images. Some of these filters do not consider the statistical characteristics of SAR images (e.g., median filter) whereas the majority of the filters consider the statistical characteristics of SAR images (e.g., lee, frost, and the gamma map filter). The later class of the filters assumes either a Gaussian distribution of the speckle noise in SAR images (e.g., Lee, Lee-Sigma, and Frost) or a Gamma distribution of the speckle noise (e.g., Gamma-Map filter) (Xiao et al. 2003). Although both filter types were tried, the Gamma-Map filter provided the best results in removing the speckle noise of the Radarsat-1 image of the study area.

The Gamma-Map filter is frequently used to remove the high frequency noise while it preserves the high frequency features of the image, such as edges. Various kernel sizes of the gamma-map filters were applied. Although numerous kernel sizes were tried, the best results (Fig. 17) were obtained by applying the 7*7 kernel size. The algorithm of the Gamma-Ma filter was developed by Lopes et al. (1993).

Data Geocoding

Once, the free-speckle radar backscattered image was created, it was geocoded using various map projection operations that are available in the PCI[®] software. These

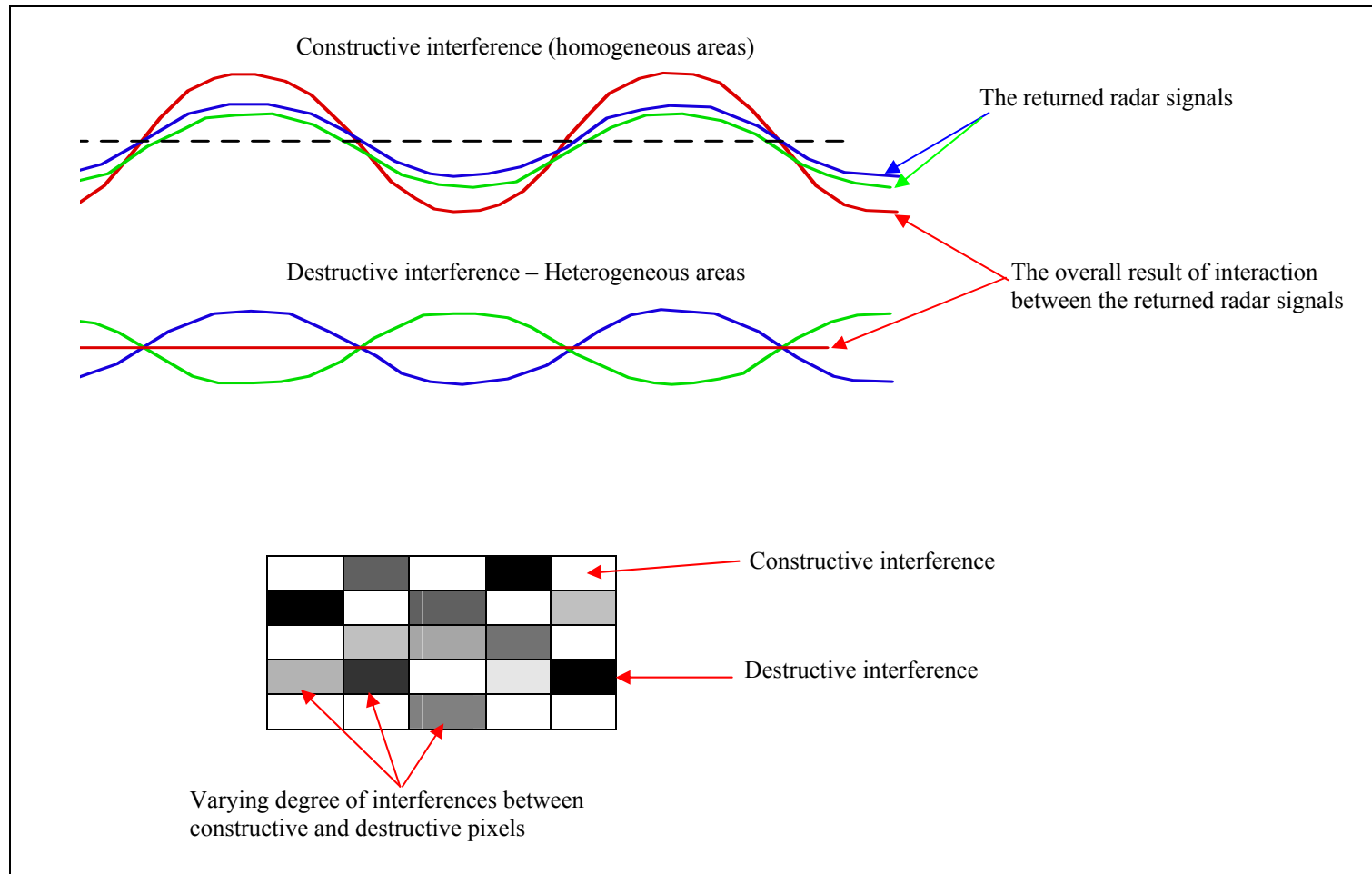
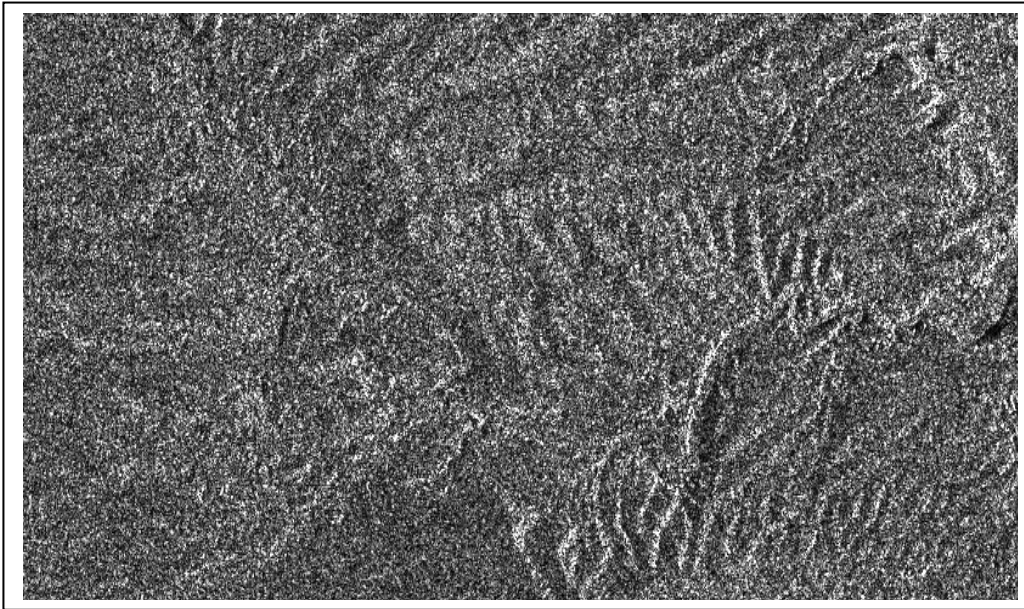
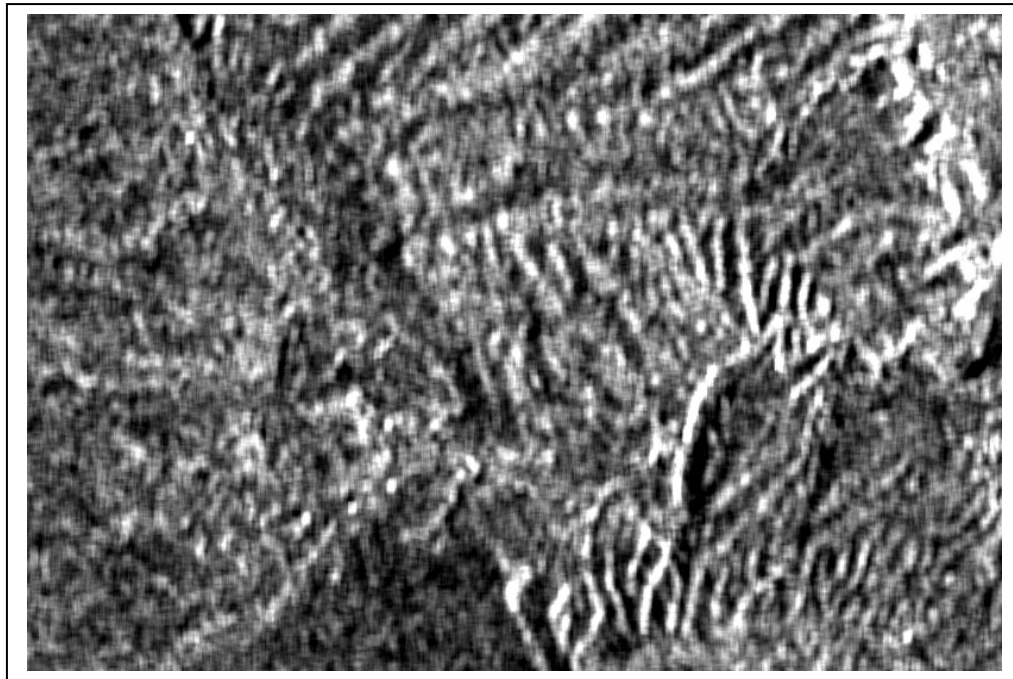


Fig. 16: The origin of speckle in radar imageries, (modified after Remote Sensing Tutorial, Canada Centre for Remote Sensing 2004).



A: An example of area without removing the speckle noise



B: The same area after applying a 7*7 kernel size of the Gamma-Map adaptive filter

Fig. 17: An example shows a Radarsat-1 image before removing the speckle (A) and after removing the speckle (B). Homogeneous areas of radar backscatter with preserved edges can be recognized in B.

operations include several steps. These steps are: 1) determining the projection parameters, 2) collecting ground control points (GCP's) from the DOQ images, and 3) resampling the radar backscatter image. The projection parameters are the UTM projection, unit meters, and the GRS 1980 datum. Ground control points were collected based on image-to-image basis. Finally, the radar backscatter image was resampled using the GCP's and the projection parameters.

Extracting Thematic Layers

The next step was to produce thematic layers. Various thematic layers were extracted from the DOQ, DEM, and the radar backscatter image. These layers are:

- ***The Main Trunk Stream Thematic Layer***

This layer involves the main trunk stream in the study area. The layer is extracted from the mosaicked DOQ image using the vector module of ERDAS[®] Imagine software. The trunk stream represents the main link between major contributing areas in the fluvial system. The trunk stream represents the local base level for the erosional processes that occur in the contributing area. In the study area there are three main reaches of the trunk stream: the upper reach, the middle reach and the lower reach. Each reach is responsible for transporting mass from one contributing area to another through a common outlet.

- ***The Thematic Layer of the Contributing Areas***

This layer is a polygon layer that is extracted from the mosaicked DOQ image. There are three major contributing regions in the study area: the upper contributing

region that is drained by the upper reach of the main trunk stream, the middle contributing area that is drained by the middle reach of the trunk stream, and the lower contributing area in the east of the study area that is drained by the lower reach of the main trunk stream. Each contributing regions is represented by a polygon and consists of various geomorphic systems.

- ***The Geomorphic Systems Thematic Layer***

Rock types, slopes, and morphological characteristics of the study area were used to define and map the boundary of various homogenous units that represent the geomorphic systems in each contributing area.

- ***The Slope Thematic Layer***

The slope of the surface is the most important topographic measure of the potential of a surface to transport mass in the landscape. The slope layer of the study area was extracted using the Slope Operation of the Spatial Analyst module available in ARCVIEW® 3.2 software. The slope was categorized using the Scholz (1972) scheme of classifying surface slopes into, slightly slopping surfaces ($0.50 - 2^\circ$), gently inclined surfaces ($2 - 5^\circ$), strongly inclined surfaces ($5 - 15^\circ$), steep surfaces ($15 - 25^\circ$), very steep surface ($25 - 35^\circ$), and precipitous ($> 35^\circ$).

Data Integration

Both the slope and the radar backscattering image are raster representations of topographic and physical characteristics of Earth's surface. A raster representation provides the capability of performing mathematical operations. The Map Algebra

operation of the Spatial Analyst extension available in the GIS ARCVIEW[®] program was used to combine the slope raster layer and the radar backscattering image. The resulting image represents an index of the connectivity potential of the study area. The image was used to study the connectivity potential of each geomorphic system in the study area and the system-wide connectivity.

Data Analysis

The Summarize Zone operation of the Spatial Analyst extension available in the ARCVIEW[®] GIS program was used to extract the mean of the connectivity index for each geomorphic system in the study area. Then, the Natural Break classification method available in the ARCVIEW[®] was used to identify the breakpoints between the various classes using a statistical operation (Jenks optimization). Using this method, the sum of the variance within each of the classes was minimized. Natural Break finds groupings and patterns inherent in the data. A twelve classified groups were set for the Natural Break operation to disclose various patterns of the connectivity potential between various geomorphic systems. Twelve classes have been grouped again to be only six groups according to their spatial distribution across the study area. These classes were used to define various levels of the connectivity potential of various geomorphic systems. These levels were then divided into the geomorphic systems that have low connectivity potential, the geomorphic systems that have intermediate connectivity potential, and the geomorphic systems that have high connectivity potential. Besides defining the connectivity potential using the connectivity index, the mean of the

connectivity index of each geomorphic system was used to evaluate the system-wide connectivity.

To study system-wide connectivity in the fluvial system as a function of the variation in the connectivity potential of various geomorphic systems, the ratios of the connectivity potential index of the upstream geomorphic system (CPI_u) to the connectivity potential index of a downstream geomorphic system (CPI_d) were calculated through the geomorphic systems of the study area. The ratio produces three states:

$CPI_u / CPI_d > 1$, $CPI_u / CPI_d \approx 1$, and $CPI_u / CPI_d < 1$.

CHAPTER V

DATA ANALYSIS

Introduction

Developing methodology for defining and mapping the connectivity potential of the landscape and its impact on the system-wide connectivity at the fluvial system scale is the main focus of this dissertation. Determining the connectivity potential of the geomorphic systems in the landscape requires analyzing important variables that influence the potential of mass movement in the landscape. The landscape gradient and the surface roughness are considered important topographic and physical quantitative measures of the potential of a geomorphic system to transport mass in the landscape. Determination and integration of these variables help analyze the connectivity potential of the various geomorphic systems. The connectivity potential is represented as an index that expresses the potential of the geomorphic system for mass movement in the landscape. The Estufa Canyon drainage basin was selected as a pioneer area to develop a methodology for determining the connectivity potential index.

Geomorphic Systems of Estufa Canyon

To study the connectivity potential of geomorphic systems in a whole drainage like Estufa Canyon, the major interconnecting spatial feature should be determined first. The trunk stream represents the major interconnecting spatial link in Estufa Canyon. The main trunk stream is divided into three major reaches: the upper reach, the middle reach, and the lower reach (Fig. 18). Each reach represents the local base level for the erosional

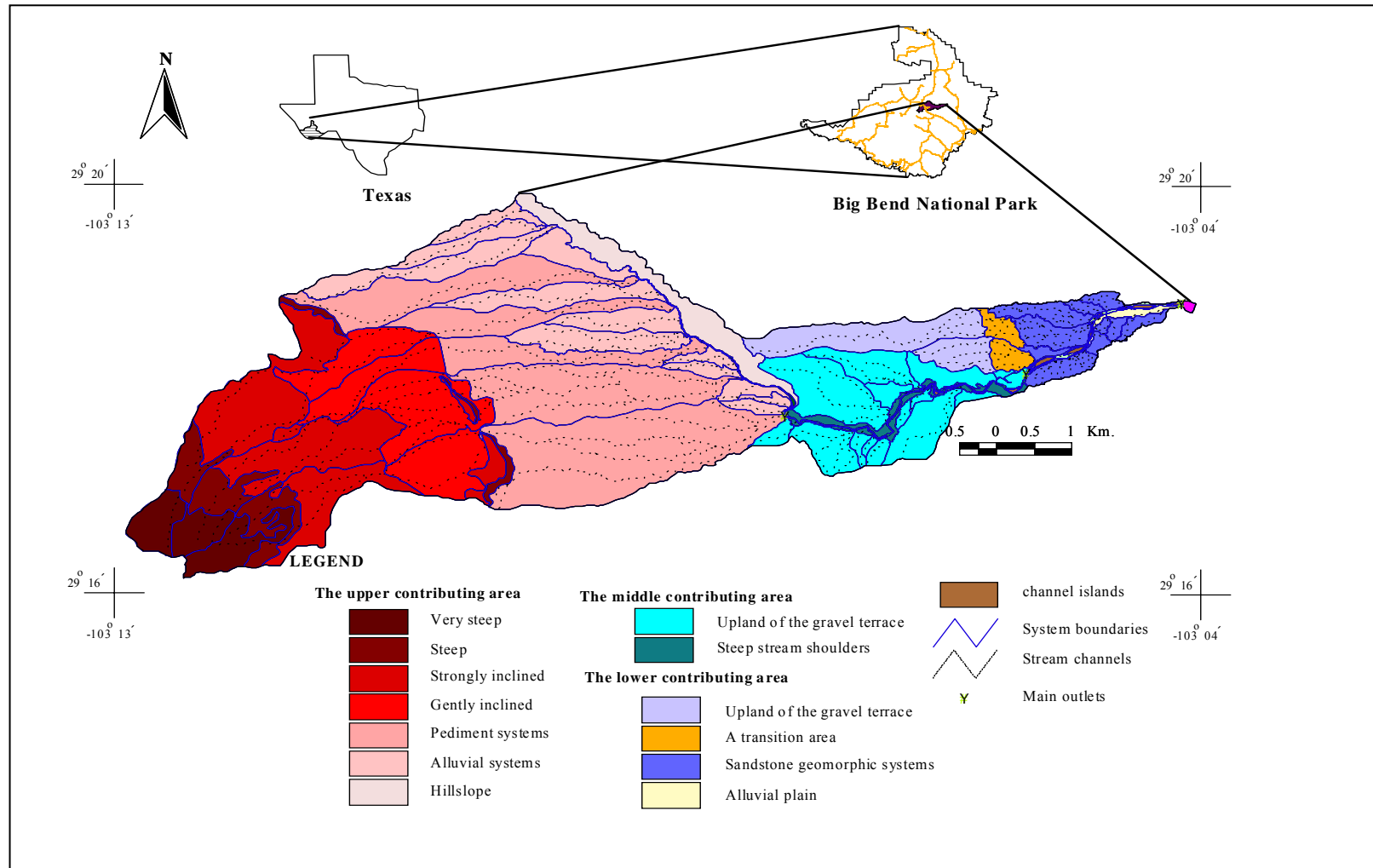


Fig. 18: Main geomorphic systems of Estufa Canyon.

processes that occur in its contributing area. Each reach transports mass from a major contributing area in the down stream direction. The upper reach transports the mass from the upper contributing area, the middle reach transports mass from the upper contributing area and from the middle contributing area, and the lower reach of the trunk stream transports mass of the lower contributing area and from the upper and the middle contributing areas (Fig. 18). Each contributing area is divided into various geomorphic systems.

In the upper contributing area, the boundaries of various slope units such as the gently inclined, strongly inclined, steep and very steep were used to define the boundaries of the geomorphic systems in the western part of the study area. These systems are flanked to the east by a wide gently inclined to slightly slopping surface of the alluvial deposits. The surface of the alluvial deposits is dissected by parallel eastward flowing deeply dissected streams. Stream channels in the alluvial deposits are separated by narrow alluvial plains. Each stream and its alluvial plain form a separate elongated geomorphic system. These system transport mass from the upstream geomorphic systems to the upper reach of the trunk stream (Fig. 18). A N-S trending narrow hillslope occurs as well along the upper reach and the hillslope is transported in the downstream direction by the upper reach of the trunk stream through a common outlet in the south central area of the study area (Fig. 18). Through this point, mass from the upper contributing area is transported into the middle contributing area.

Examination of Fig. (18) shows that the middle contributing area is more homogeneous in rock composition and slope than the upper contributing area. The

majority of the middle contributing area is characterized by strongly inclined surfaces. There are two main units that can be defined in the middle contributing area of the study area. These units are the upland small drainage basins and the steep slopes along the middle reach of the trunk stream (Fig. 18). In addition to mass that is transported by the upper reach of the trunk stream, the middle reach of the trunk stream transports mass from these geomorphic systems to the lower reach of the trunk stream.

In addition to mass that is transported from the upper contributing area and the middle contributing area, the lower reach of the trunk stream transports mass from the lower contributing area. The dominant slopes in the lower contributing area range from slightly sloping, gently inclined, to strongly inclined. The lower contributing area is characterized by the presence of two main areas: the gravel dominated area and the sandstone dominated area. Both the areas are separated by a transitional area of steep slopes (Fig. 18). Both of the gravel dominated area and the sandstone-dominated area are composed of small drainage basins. A narrow alluvial plain occurs along the southern bank of the lower reach of the trunk stream.

Defining the major geomorphic systems, e.g. the contributing areas, and their components, e.g. various geomorphic systems, represent the first step for determining the connectivity potential of various geomorphic systems in the landscape by analyzing the landscape gradient and surface roughness.

The Landscape Gradient

The landscape gradient was calculated from a 30 meter DEM using the Slope Operation of the Spatial Analyst extension available in the ARCVIEW[®] GIS program (Fig. 19). To study the influence of the landscape gradient on the connectivity of a geomorphic system, the magnitude of the slope within the geomorphic systems and the rate of changes of the slope between these systems is considered. The magnitude of the slope determines the relative potential of the geomorphic system to transport mass in the landscape whereas the change in the slope is useful in determining the system wide connectivity in the whole fluvial system.

The landscape gradient in the study area is characterized by high changes; both in the magnitude and in the spatial distribution. In the western part of the study area, the precipitous slopes change to very steep, steep and strongly inclined. The strongly inclined slopes are flanked in an eastward direction by the area of the alluvial deposits. The slope of the alluvial deposits fluctuates between slightly sloping to gently inclined surfaces. These surfaces express a pattern of narrow NE-SW alternating belts of gently inclined to slightly sloping surfaces. These belts represent active erosional surfaces (Fig. 19). Toward the outlets of the area of the alluvial deposits at the south central part of the study area, the slope suddenly increases in the middle and the lower contributing areas.

The middle contributing area is dominated by a strongly inclined surface. The slopes of the lower contributing area vary from strongly inclined surface in the gravel dominated area to a mixed surface of strongly inclined and gently inclined slopes in the

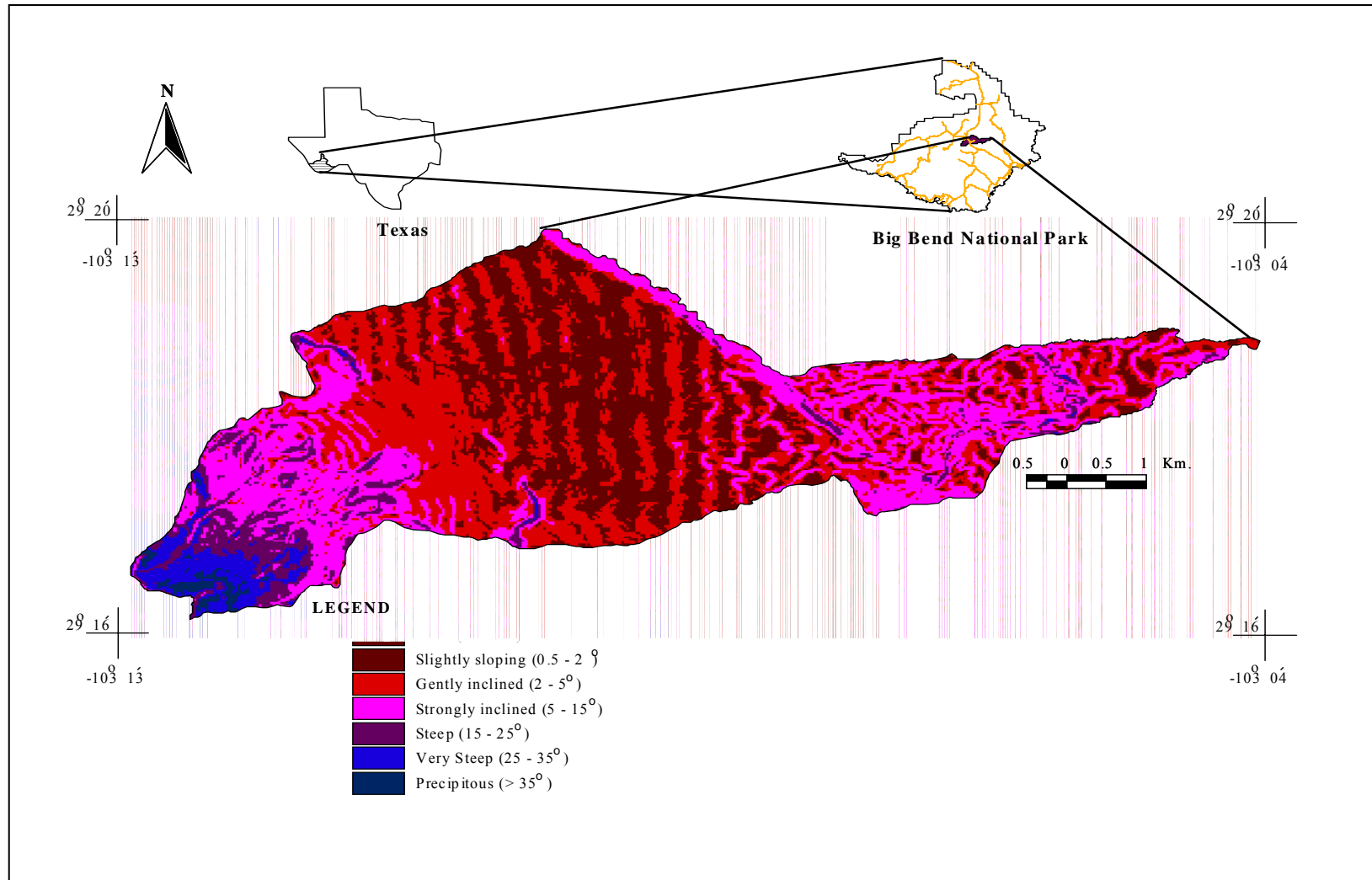


Fig. 19: The landscape gradient of Estufa Canyon.

sandstone-dominated area of the lower contributing area. An abrupt change in the slope occurs between the gravel dominated-area and the sandstone dominated-area. The transition area has a strongly inclined surface with areas of steep slope. Along with the magnitude of the slope, the spatial variations of the slopes between the geomorphic systems affect the connectivity potential of a geomorphic system. The higher the rate of change, the higher the connectivity potential between the various geomorphic systems in the landscapes.

In the downstream direction of the study area and over a total distance of ~ 15 km, the rate of change in the slopes is considerably high and varies from the upstream geomorphic systems in the western part of the study area to the downstream geomorphic systems in the eastern part of the study area through a wide surface of alluvial deposits in the middle of Estufa Canyon (Fig. 20). The landscape gradient of the upstream geomorphic systems varies from 27.5° to 5.5° over a short distance of ~ 4 Km with a rate of change $5^\circ/\text{km}$. This high rate provides the upstream geomorphic systems with a high potential energy to transport mass by stream channels to the area of the alluvial deposits in an eastward direction through a steep transition area. The rate of change in the transition area ranges from 7.5° to 2.5° over 1 km. The lowest rate of change occurs in the area of the alluvial deposits where the slope varies from 2.5° at the K-Bar Range to 5.0° at the outlet of the upper contributing area over a total distance of ~ 4.00 km. The rate decreases from the K-Bar Range area to the middle of the area of the alluvial deposits and then increases slightly again to attain the maximum increase at the outlet of the area of the alluvial deposits (Fig. 20).

From the outlet of the upper contributing area to the main outlet of Estufa Canyon, the rate of change between the geomorphic systems ranges from 7.5° to 5.0° over a distance of 3° Km in the middle contributing area. This rate is higher than that in the area of the alluvial deposits. A steep transition occurs between the middle contributing area and the lower contributing area with a high rate of slope change. The rate of slope change in the transition area ranges from 7.50° to 2.5° over 1 Km. The rate of change of the slopes between geomorphic systems greatly affects the connectivity potential of each geomorphic system, from one side, and the system-wide connectivity in the whole fluvial system, from another side.

In Estufa Canyon, the high magnitude and the high rate of change of the slopes in the upstream geomorphic systems are responsible for rapid mass transportation by stream channels to the area of the alluvial deposits. Generally, the geomorphic processes in the area of the alluvial deposits function in the landscape either as a depositional or as a transitional erosional geomorphic process. Being a depositional environment or an erosional one is, basically, a function of the changes in the slopes of the downstream geomorphic systems that are flanking the pediment surface. High slope changes in the downstream geomorphic systems result in maximizing mass movement in the alluvial deposit surface. Maximizing mass movement allows the area of the alluvial deposits to function as an erosional transitional system in the whole fluvial system. The lower the changes of the slopes in the downstream geomorphic systems results in minimizing the downstream mass movement in the area of the alluvial deposits system. The area of the

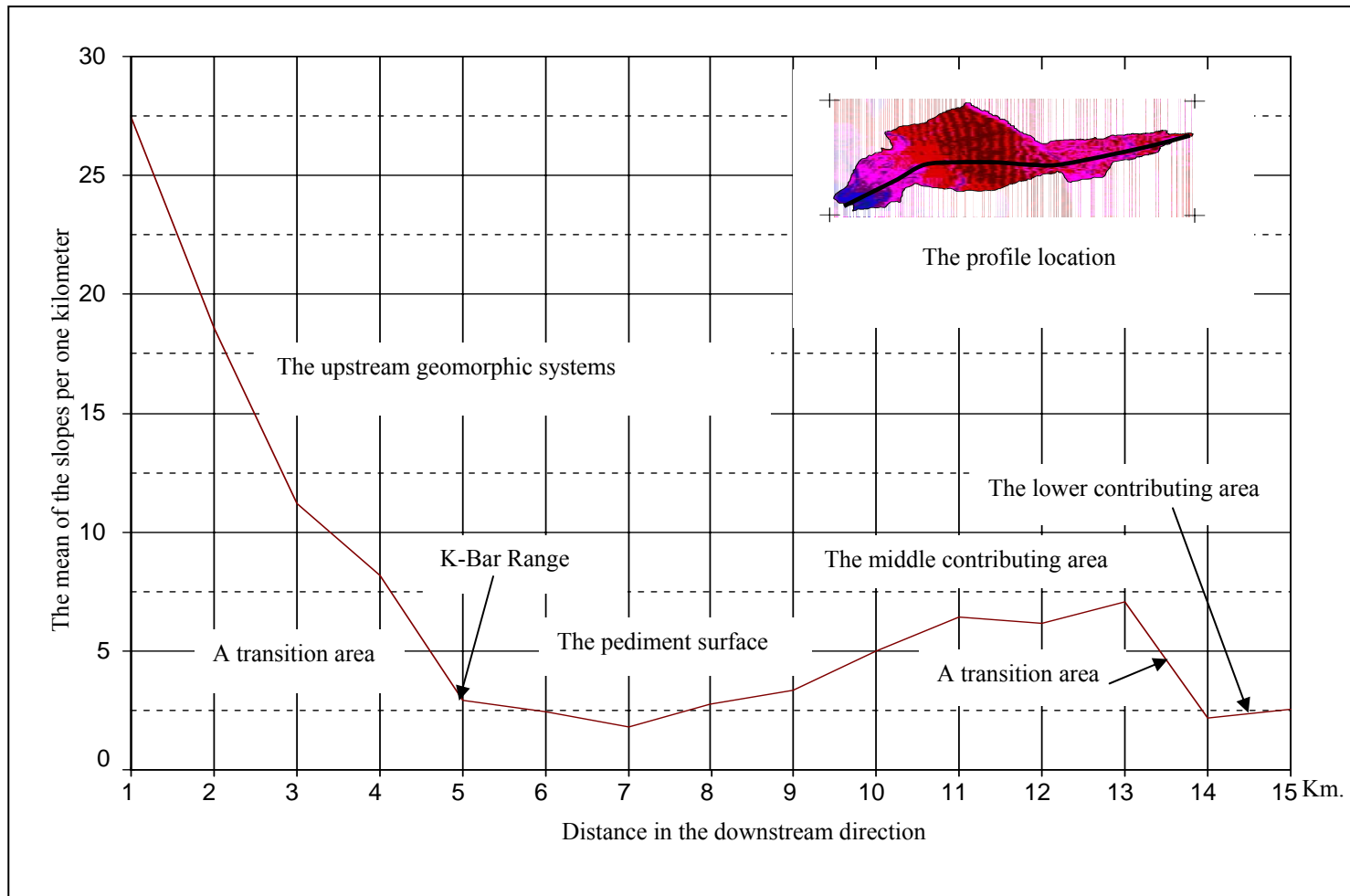


Fig. 20: A graph showing the rate of changes in the landscape gradients in the downstream direction of Estufa Canyon.

alluvial deposits in this case tends to function as a depositional system.

The erosional nature of the area of the alluvial deposits in the study area is shown by the absence of depositional landforms such as alluvial fans and bajadas. This erosional nature tends to maximize mass movement in the western part of the study area and accordingly, the connectivity potential of the upstream geomorphic systems in this part of the study area. To understand the overall response of the whole fluvial system to the external environmental perturbations, one must understand the processes and interactions between various geomorphic systems. Another parameter that can be used to analyze the connectivity potential of each geomorphic system and the whole fluvial system is the surface roughness.

The Surface Roughness

Unlike the optical remote sensing systems where the reflection is a function of the chemical composition of Earth's surface, the reflection of radar microwave radiation from Earth's surface is a function of various surface physical characteristics. These characteristics include the surface roughness and the dielectric properties. Surface roughness is one of the most important characteristics of the target that influences the radar backscattering. Surface roughness can be considered at three scales: microscale roughness, mesoscale roughness, and macroscale roughness. Whereas the mesoscale and the macroscale roughness deal with the textural and topographic variations of Earth's surface, the microscale roughness represents the tonal variations in radar images (Lewis and Henderson 1998). The tonal variations in radar images express the "smoothness" of

the surface. The focus in this dissertation is placed on the microscale surface roughness that expresses the influence of grain size variations on the intensity of the radar backscattering.

To understand the surface roughness from radar remote sensing perspectives, it is critical to review the radar equation. The transmitted energy from the radar antenna impinges the target of a cross-section area, σ , according to the following equation (Moore 1970):

$$P_r = \frac{P_t}{4\pi R^2} G_t \sigma \frac{G_r \lambda^2}{4\pi^2 R^2} \quad (10)$$

where,

- P_t the transmitted power,
- P_r the returned power,
- G_t the transmitted antenna power gain,
- G_r the receiving antenna power gain,
- σ the radar scattering cross section of the target,
- R the range between the target and the radar, and
- λ the incident wavelength.

This equation is formulated for an isolated target with a cross-section area, σ (Ulaby 1982). To apply the equation on an extended target of an area (A), the concept of an average radar scattering cross-section per unit area, σ^o , should be applied. The radar equation, then, take the following form:

$$P_r = \frac{P_t}{4\pi R^2} G_t \sigma^o A \frac{G_r \lambda^2}{4\pi^2 R^2} \quad (11)$$

$$\sigma^o = \frac{P_r (4\pi^3 R^4)}{P_t G_t G_r \lambda^2} \times \frac{1}{A} \quad (12)$$

The equation shows that the backscatter coefficient, σ^o , is a function of both the wavelength of the radiation and the incident angle. The backscatter coefficient, σ^o increases as the wavelength and the incident angle decrease. At a given wavelength, the backscatter coefficient depends basically on the surface roughness and the incident angle.

The surface roughness refers to variations in the grains size of targets on the surface (Fig. 21). Various approximations have been proposed to identify the roughness of the target based on the relationship between its size and the wavelength of the radiation. The “rule of thumb” is $\lambda/10$ to identify the surface roughness. The surface is rough, for example, if it has a size of 0.56 cm or larger in the case of using the Radarsat-1 image of “C” band that has a wavelength of 5.6 cm. Another approximation for estimating the surface roughness is the Rayleigh Criterion. In this approximation, the

average height variation of a target is compared with the wavelength “ λ ” of the radar radiation and the looking angle “ θ ” using this equation

$$h_{rms} > \frac{\lambda}{8 \cos \theta} \quad (13)$$

Having the look angle of 37.09 and the wavelength of the 5.6 for a Radarsat-1 image, the surface is considered rough if it has a size of 0.88 cm. A surface that has grain sizes less than 0.88 cm is considered smooth surface. A more sophisticated method that is used to identify various roughness classes based on the wavelength and the look angle is proposed by Peake and Oliver (1971). In this method, three classes of the surface roughness can be recognized: rough, intermediate and smooth. A target is considered smooth when:

$$h_{rms} > \frac{\lambda}{25 \cos \theta} \quad (14)$$

and a target is considered rough when

$$h_{rms} > \frac{\lambda}{4 \cos \theta} \quad (15)$$

Using Radarsat-1 wavelength and the look angle, the surface is considered smooth if it has grain size 0.28 cm and rough if it has a grain size of 1.76 cm. Values between these limits are considered intermediate. The above-mentioned approximation discloses the sensitivity of the radar data to recognize grains sizes of pebble size (0.2 cm

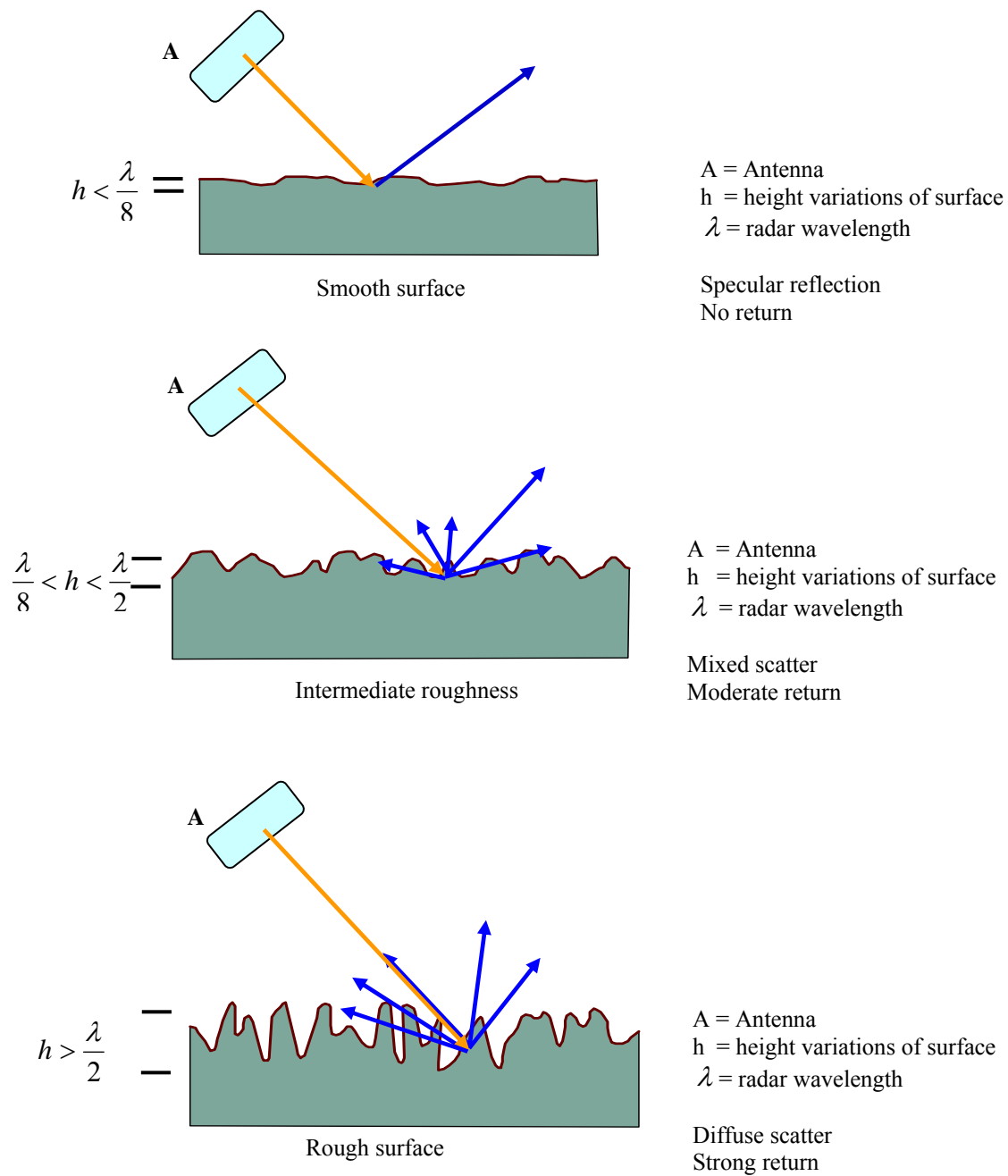


Fig. 21: A graph showing the relationship between the size of the object, wavelength, and intensity of backscattering (modified after Natural Resources Canada, Canada Center for Remote Sensing, 2004).

to 6.4 cm) and larger. To produce a map of detailed surface roughness, the grain size variations are measured in selected locations of a given area using special equipment. Then, a linear regression analysis is carried out to build a correlation model expressing the relationship between the backscattering coefficient and the grain size variations in a study area. Finally, the model is used to produce a surface roughness map in cm scale from the backscattering data in the radar image. In this research, the backscattering coefficient was used as a surrogate for the surface roughness in the study area. Bright areas mean that a larger proportion of the transmitted radar radiation is bounced back to the radar-receiving antenna, e.g., high backscattering coefficient. A high backscattering coefficient reflects the presence of rough surfaces. On contrast, darker areas mean that a smaller proportion of the transmitted radar radiation is bounced back to the radar antenna, e.g., low backscattering coefficient. A low backscattering coefficient indicates the presence of smooth surfaces. Thus, the values of the backscatter coefficient, σ^0 , are indications of the degree of surface roughness in the terrain. Assuming that the surface roughness in the study area is attributed mainly to the grain size variations, the backscattering coefficient, can be used to express variations in the grain size of the study area.

The backscattering coefficient, σ^0 , for the study area was extracted from the SGF Radarsat-1 data product using the Sarsigm module available in the PCI[®] digital image processing software (Fig. 22). The values of the backscattering coefficient, σ^0 , were calculated using the amplitude scale not a dB scale; thus, the calculation of the mean for

each geomorphic system is doable. The image of the backscattering coefficient reflects the magnitude and the spatial variations of the surface roughness in the study area.

The mountainous area in the western part of the study area is characterized by a bright tone. It has the highest values of the backscattering coefficient, σ^0 , in the study area. These bright areas represent the steep slopes that are covered by coarse fragments such as boulders, cobbles, and gravels (Fig. 22). The bright tone decreases gradually in an eastward direction where the slope decreases. In the area of the alluvial deposits, the tone becomes a possible mixture of dark and light areas indicating a mixed effect of shrubs and gravely sandy soil (Fig. 22). To the east of the area of the alluvial deposits, high terrace gravels are characterized by various surface tones. The high-level gravel terrace can be divided into two main areas: one adjacent to the area of the alluvial deposits and another one that occurs at the outlet of the study area.

Between these two areas, a steep slope surface occurs. The area adjacent to the alluvial deposits is composed mainly of gravel (Fig. 22) whereas the area at the outlet is composed mainly of sands. The former has a brighter surface in the image than the later. Between those areas, a NW-SE trending steep slope area occurs with a brighter tone. Overall, the image of the backscattering coefficient, σ^0 , displays high variations of surface roughness in the study area.

Data Integration

Gravity is an important driving force affecting the geomorphic processes in the landscape. The landscape gradient controls the gravitational forces that influence the

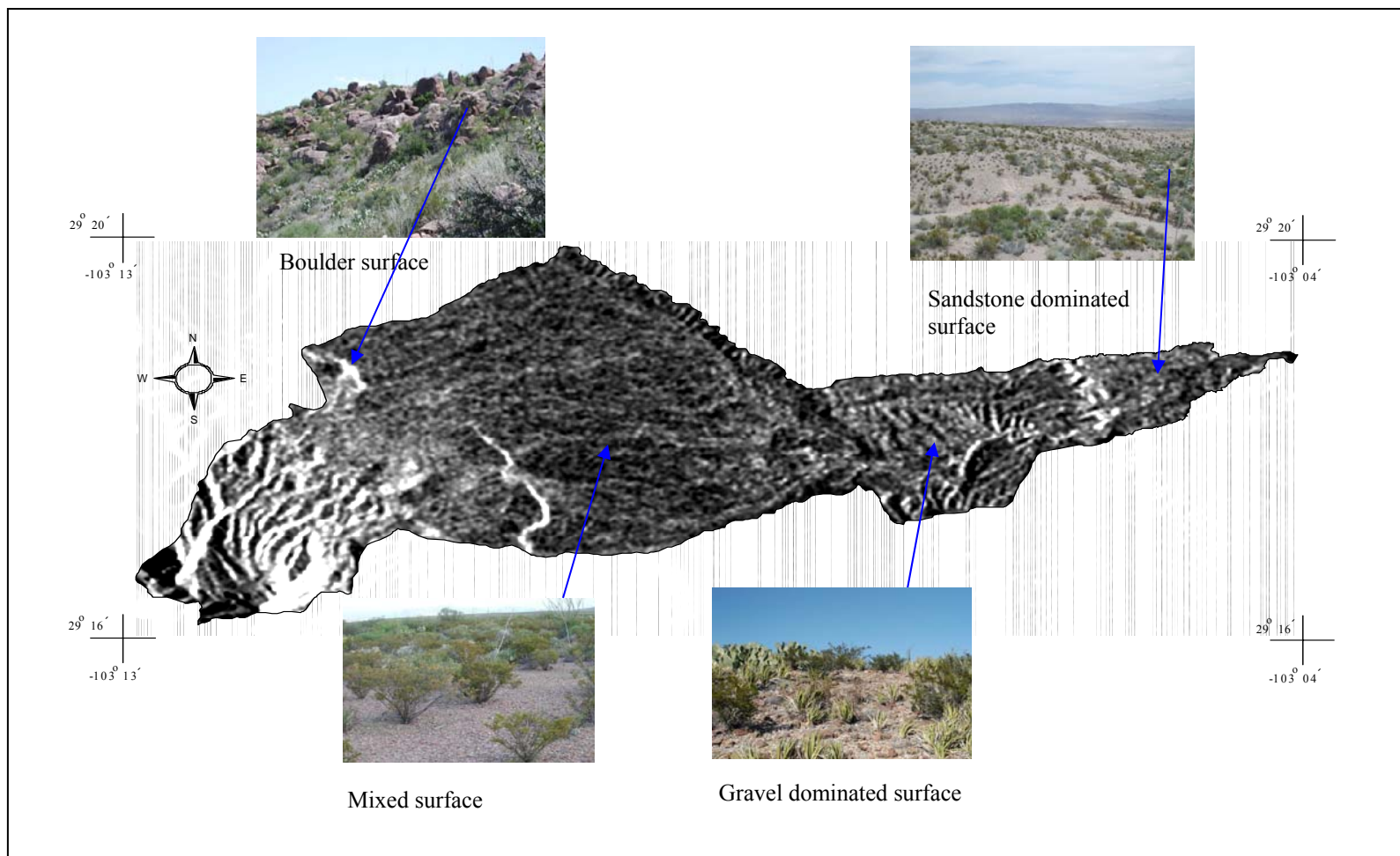


Fig. 22: A Radarsat-1 image showing the variation of the backscattering coefficient over various roughness surfaces.

surficial materials on various landscape slopes. The relationship between the grain size and landscape gradient has received considerable attention (Lawson 1915, Bryan 1973, Church 1992, and Lancaster 2002). In an arid climate, constant slopes occur in areas that consist of one rock type (Bryan 1973). This statement implies that the spatial variation of slopes in the landscape is highly related to the spatial variabilities of rock types for a given climatic setting. In a desert environment, the hard rocks are characterized by large fragments that occur on the steep slopes whereas fine fragments occur on the low slopes (Lawson 1915). In river systems, the main transporting agent is the channel system. The variations of stream power, which is a function of the landscape gradients, affect the spatial distribution of the grain size in the fluvial system (Fig. 23). The coarse fragments occur in the upstream areas where stream power is high. The fine particles occur in the downstream areas of the fluvial system where the stream power is low. Between the coarse fragments in the upstream areas of the fluvial system and the fine fragments in the downstream areas of the fluvial system, a wide range of grain size variations occur. The radar backscattering coefficient is used to express these variations. Analyzing the surface roughness and the landscape gradient is important to evaluate the potential of various geomorphic systems to transport mass through the landscape.

The rate and the velocity of water or other mass movement in the landscape are a function of the landscape gradient and the textural characteristics of mass (Etzelmuller 2000). Thus, analyzing the surface roughness and the slopes of the landscape can help in the understanding of the potential of a geomorphic system to transport mass. Geomorphic systems that have high surface roughness and high slopes are assumed to

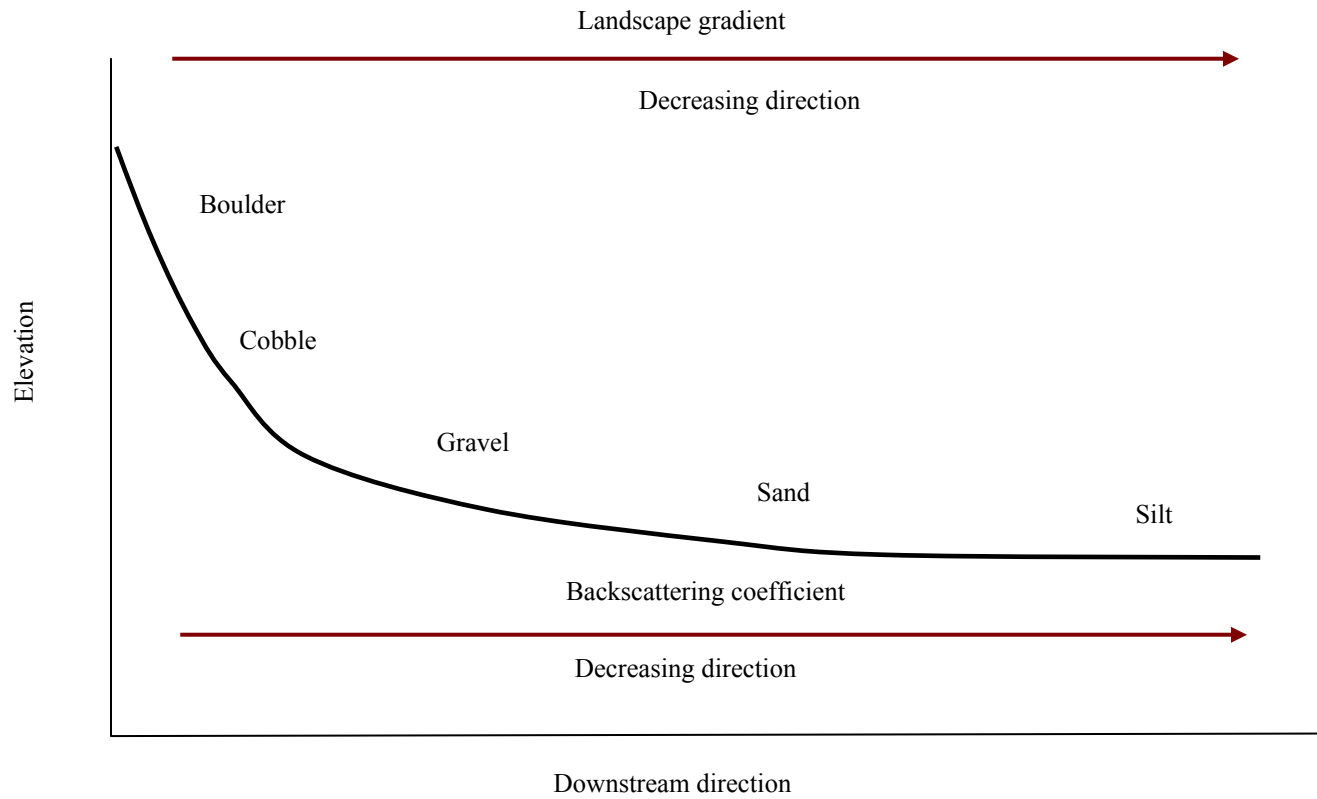


Fig. 23: The relation between the landscape gradient and the particle size distribution in the downstream direction (modified after Church 1992).

have high potential for mass movement. On the other hand, geomorphic systems that have low surface roughness and low slopes are assumed to have low potential of mass movement. The higher the potential of the geomorphic system to transport mass, the higher the connectivity potential the geomorphic system has. On the other hand, the lower the potential of the geomorphic to transport mass, the lower the connectivity potential of this system. Thus, combining both the slope and the surface roughness can produce an index of the connectivity potential of various geomorphic systems in the landscape.

In the study area, the connectivity potential of a geomorphic system has been evaluated using the integration between the surface roughness and the landscape gradient. The relationship between the surface roughness and the landscape gradient displays a positive, significant correlation of $R^2 = 0.525$ (Fig. 24). The intermediate correlation coefficient discloses that the surface roughness and the landscape gradients are not completely correlated over the whole study area. This intermediate correlation coefficient might be attributed to the spatial variabilities of the surface roughness over various geologic surfaces in the study area. The spatial variabilities between the surface roughness and the landscape gradients can be integrated to analyze the connectivity potential of the geomorphic systems in the study area. The integration between the surface roughness and the landscape slopes can be used to develop a connectivity index of the potential of various geomorphic systems for transporting mass in the study area.

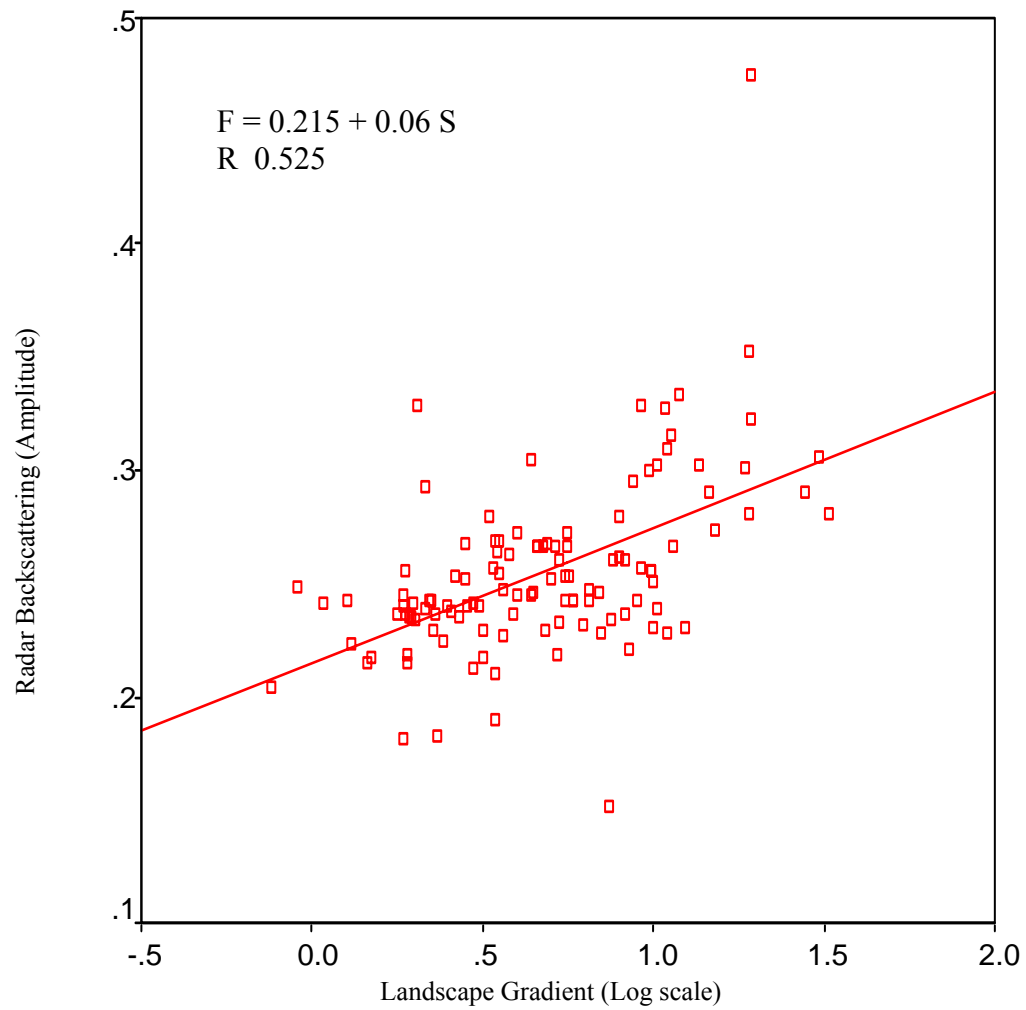


Fig. 24: The relationship between radar backscattering and the landscape gradient.

Analyzing the Connectivity Potential of the Geomorphic Systems

Integration of data from various sources is a strength of a GIS system. Integration of landscape gradients that are extracted from a DEM of 30 m spatial resolution and the surface roughness that is extracted from Radarsat-1 image can help in defining and mapping various classes of the connectivity potential of geomorphic systems.

Assuming constant conditions of geology, vegetation, and climate, the connectivity potential can be analyzed as a function of the spatial variabilities of the slope and the surface roughness. The advantage of combining these layers is that both represent measurements of important characteristics of the landscape. In addition, both the landscape gradient and the surface roughness are represented in a raster digital format, which facilitates mathematical operations. If one assumes a constant condition for other parameters in a geomorphic system, the connectivity potential can be expressed as the following:

$$C_p = K * S (1-F) \quad (16)$$

where:

C_p is the index of the connectivity potential,

F is the surface roughness,

S is the slope, and

K is the constant that depends on geology, vegetation, climate, etc.

The combination of the raster layers of the slope and the surface roughness produces an image that represents an index of the connectivity potential of the landscape (Fig. 25). The lower values represent areas of low connectivity potential whereas the higher values represent areas of high connectivity potential. The combined image provides an index of the connectivity potential for various geomorphic systems that form Estufa Canyon.

The Summarize Zone operation of the spatial analyst extension that is available in the ARCVIEW® GIS program extracts the mean of the connectivity potential index (CPI) for each geomorphic system from the connectivity index image. The Natural Break classification method available in ARCVIEW® is used to identify the breakpoints between the various classes using Jenk's optimization method. Although this method is rather complex, it minimizes the sum of the variance within each of the classes. The natural Break method finds groupings and patterns inherent in the data. A twelve classified group was established for the Natural Break operation to disclose various patterns of the connectivity potential between various geomorphic systems in the study area. The twelve classified groups were then reduced to six groups according to their spatial distribution across the study area (see figure on page 95). The six groups include:

- ***Geomorphic Systems of Low Connectivity Potential***

These systems have the lowest values of slope and the surface roughness reflecting low connectivity potential for mass movement. The CPI of the systems ranges from 0.191 to 0.755. These systems are located on the alluvial deposits area.

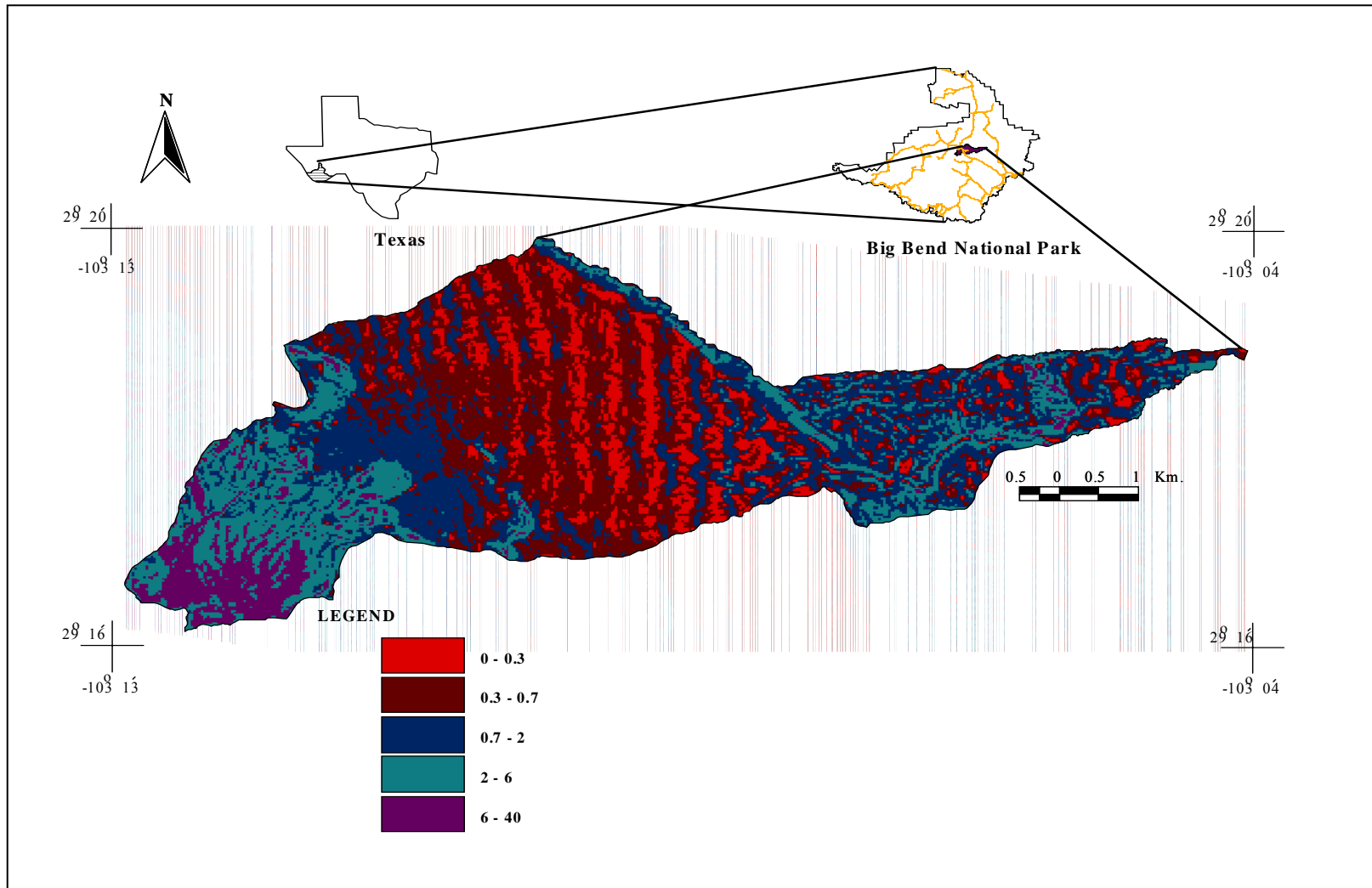


Fig. 25: A map showing the spatial variation in the connectivity potential index of Estufa Canyon.

They can be classified into two classes: very low connective geomorphic systems and low connective geomorphic systems. The CPI ranges from 0.191 to 0.478 for the very low connective systems and from 0.478 to 0.755 for the low connective geomorphic systems. The first is located in the middle of the alluvial deposits area whereas the second is located in the north and the south borders of the area of the alluvial deposits. The relative high connectivity potential in the north and the in the south of the area of the alluvial deposits may be related to the closeness of these systems to the outlet of the area of the alluvial deposits, such as the geomorphic systems in the south, or the short length between the source rocks and the upper reach of the trunk stream, such as the north geomorphic systems of the area of the alluvial deposits.

- ***Geomorphic Systems of Intermediate Connectivity Potential***

The geomorphic systems of this group have a CPI that ranges from 0.755 to 2.029. These systems have intermediate values of the slope and the surface roughness in the study area. These systems can be classified into two main classes: the first class has a low CPI that ranges from 0.755 to 1.130 and the second class that has a CPI ranging from 1.130 to 2.029. The first class occurs at the transition area between the geomorphic systems of the sources rocks in the western part of the study area and the surface of the area of the alluvial deposits. It represents a transition area between the geomorphic systems of high connectivity potential in the western part of the study area and the geomorphic systems of low connectivity potential in the area

of the alluvial deposits. The second class of the intermediate geomorphic systems occupies the majority of the middle and the lower contributing area in the study area.

- ***Geomorphic Systems of High Connectivity Potential***

These systems have the highest values of slope and surface roughness in the study area. They have the highest values of the connectivity potential in the study area. The CPI values range from 2.029 to 9.662. These systems can be classified into two main classes: high connective geomorphic systems with a CPI that ranges from 2.029 to 4.759 and very high connective geomorphic systems with a CPI that ranges from 4.759 to 9.662. The first class is located along the middle reach of the trunk stream and at the transition area between the gravel denominated and the sand dominated areas in the lower contributing area of the study area. In addition, these systems occupy a large area in the western part of the study area. The second class is very high connective geomorphic systems. These systems have the highest values of the slope and the surface roughness and have the highest potential of connectivity potential.

The above-mentioned classification defines the relative connectivity potential of the various geomorphic systems in the study area. Areas of high connectivity potential are characterized by high potential of mass movement whereas areas of low connectivity potential are characterized by low potential of mass movement. Examining the map of the connectivity potential distribution, it is evident that the spatial distribution of the connectivity potential is not regular. It fluctuates from high in the western part of the study area, intermediate between the source rocks and the surface of the alluvial

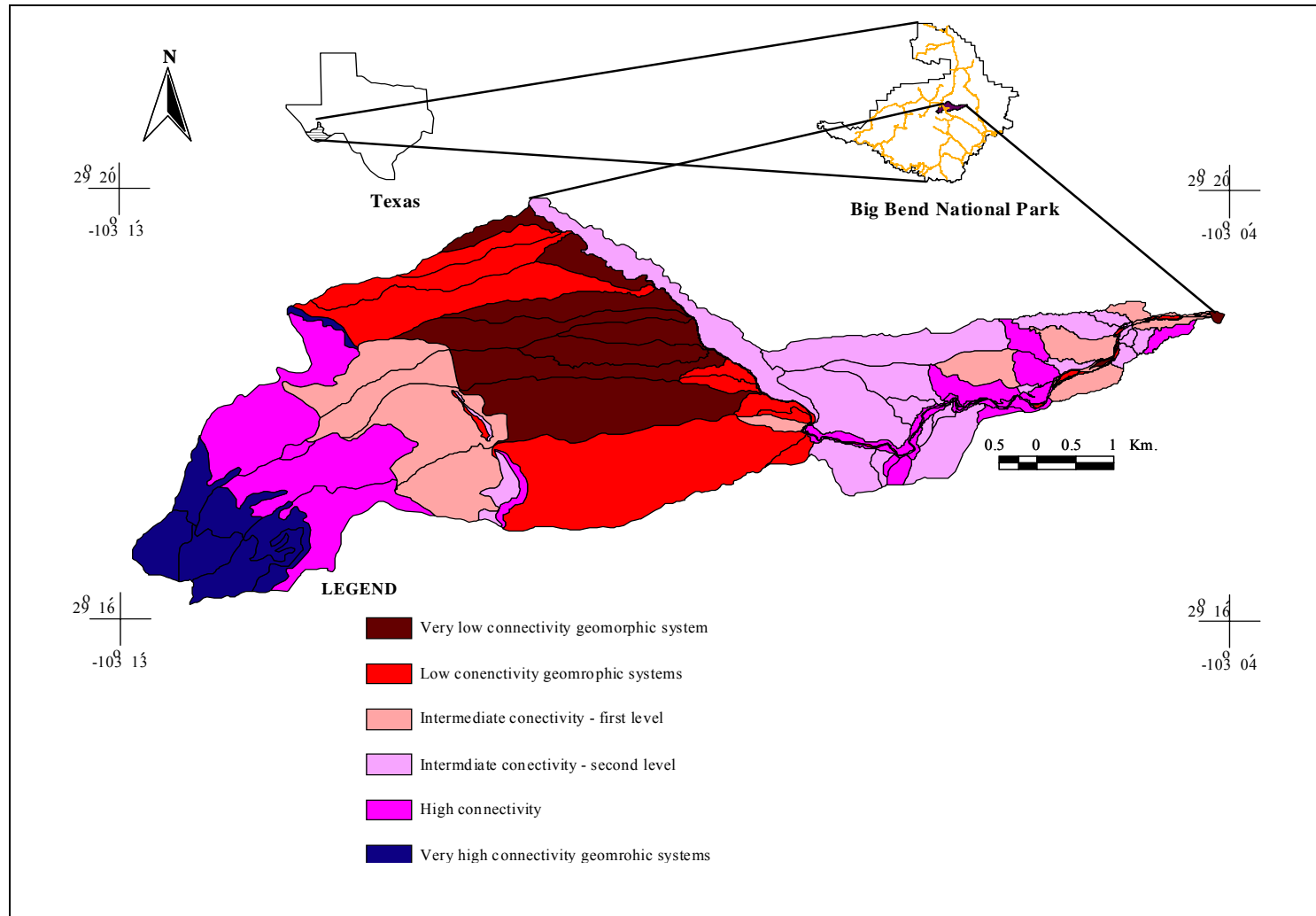


Fig. 26: The connectivity potential index of various geomorphic systems of Estufa Canyon.

deposits, to low in the middle of the study area, and then intermediate and high again in the eastern part of the study area. This pattern of spatial changes in the connectivity potential is expected to result in process connectivity between various geomorphic systems in the whole fluvial system in the study area. In the process connectivity, it is possible that a geomorphic system with a particular CPI functions to maximize or minimize mass movement in the contiguous geomorphic systems. Maximizing or minimizing mass movement because of the process connectivity results in system-wide connectivity.

System-Wide Connectivity

Laszlo (2003) introduced a new paradigm that explains the connectivity between various correlated parts of a system. In this paradigm, the connectivity in a system implies a quasi-instant correlation between various parts of that system. The quasi correlation implies, in turn, a system-wide connectivity. The system-wide connectivity requires the presence of an interconnecting medium between various system components. The interconnecting medium can be represented by the gravitational force between system components. Applying this paradigm might help understand the connectivity between various geomorphic systems that control the overall dynamic of a fluvial system.

In the fluvial system, the geomorphic systems are linked together through various spatial links. Mass movement from one geomorphic system to another geomorphic system is a function of the difference in the potential energy between geomorphic systems in the landscape. From the upstream geomorphic systems, where the potential

energy is maximum, to the major outlet of the fluvial systems, where the potential energy is minimum, the potential energy of geomorphic systems varies considerably. The amount and the trend of variation in the potential energy from one geomorphic system to another geomorphic system influence system-wide connectivity of the fluvial system.

To study system wide connectivity in the fluvial system as a function of the variation in the potential energy of various geomorphic systems, the ratios of the connectivity potential index of the upstream geomorphic system (CPI_u) to the connectivity potential index of the downstream geomorphic system (CPI_d) were calculated through the study area. The ratio produces three states: values of $CPI_u / CPI_d > 1$, values of $CPI_u / CPI_d \approx 1$, and values of $CPI_u / CPI_d < 1$. System-wide connectivity can be analyzed using these ratios.

The ratios that are higher than the unity indicate a downstream mass transportation under the influence of gravity. As the values increase, the difference in the potential energy between geomorphic systems increases resulting in high connectivity potential under the influence of the gravitational forces. In this case, the transportation rates exceed the depositional rates. The system has the lowest state of entropy at this moment (Fig. 27). As the ratio approaches unity, the transportation rates decreases and the depositional rate increases. Ratios that have values approximating unity suggest the presence of low difference in the potential energy between the upstream geomorphic system and the downstream geomorphic system. A continuous decrease in the ratio results in extra decrease in the energy difference between the upstream geomorphic

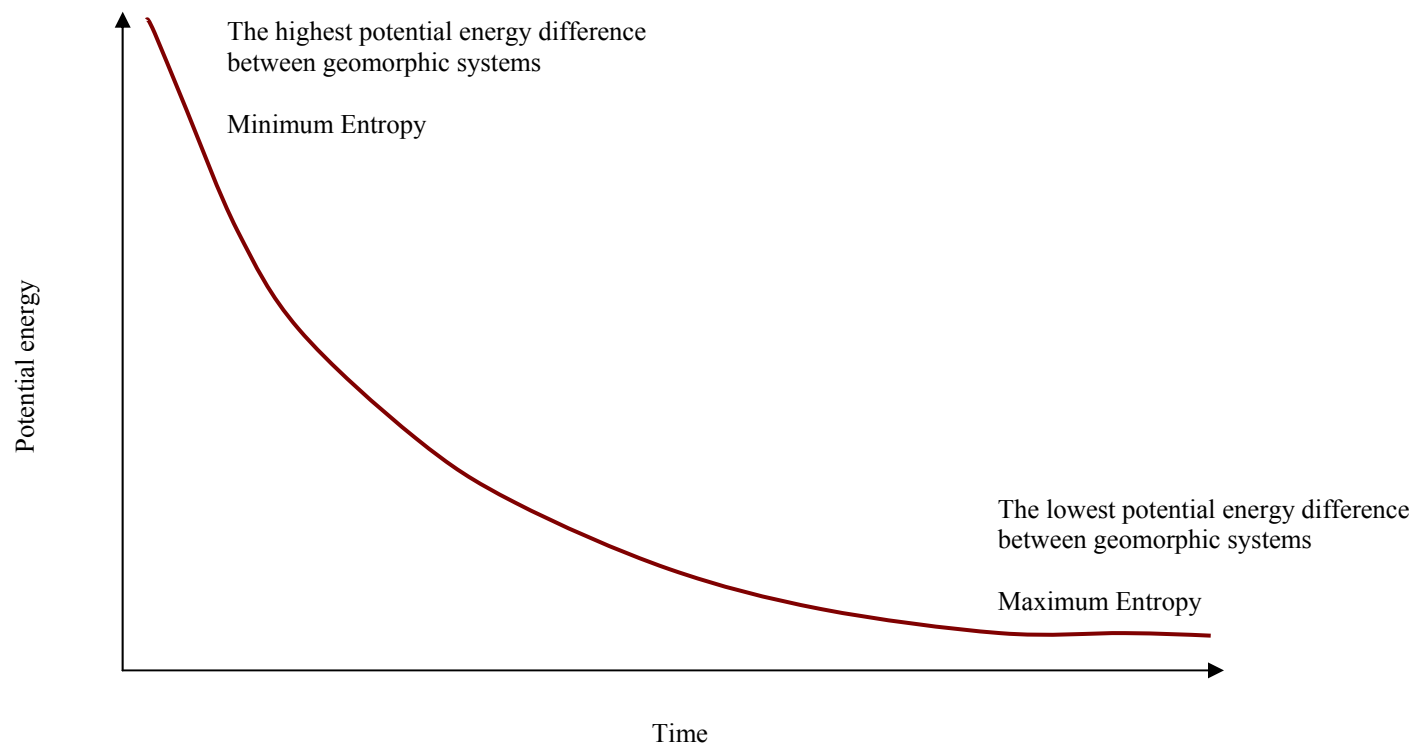


Fig. 27: The relationship between the potential energy and system dynamic.

system and the downstream geomorphic system. Then, the system approaches the optimum condition of maximum entropy (Fig. 27). At maximum entropy, continuous deposition results in high elevation in the downstream geomorphic systems. The increasing elevation in the downstream geomorphic systems leads to suppressing (i.e., minimizing) mass transportation in the upstream geomorphic systems. The system-wide connectivity under this condition is minimized. Because landscapes tend to be complex, the spatial changes in the potential energy occur on a random basis. The potential energy fluctuates between high and low values in a complex landscape. Then, the ratio may be changed to be less than unity. Ratios that are less than unity indicate that the potential energy of the downstream geomorphic system is higher than the potential energy of the upstream geomorphic system. In this case, the downstream geomorphic systems function to maximize mass movement in the upstream geomorphic systems. As the ratios become smaller, the influence of the downstream geomorphic system on mass movement of the upstream geomorphic system is maximized. The system develops minimum entropy conditions (Fig. 27), and the system-wide connectivity tends to increase. Thus, a fluvial system with high spatial variations in potential energy develops high system-wide connectivity than systems that have low spatial variations in potential energy. This view is applied to the study area to determine the system-wide connectivity.

In the study area, the ratio at “B” represents the highest values (Fig. 28). At this location, mass transportation from the upstream geomorphic system to the downstream geomorphic system is maximum. A decrease in the ratio occurs between the intermediate

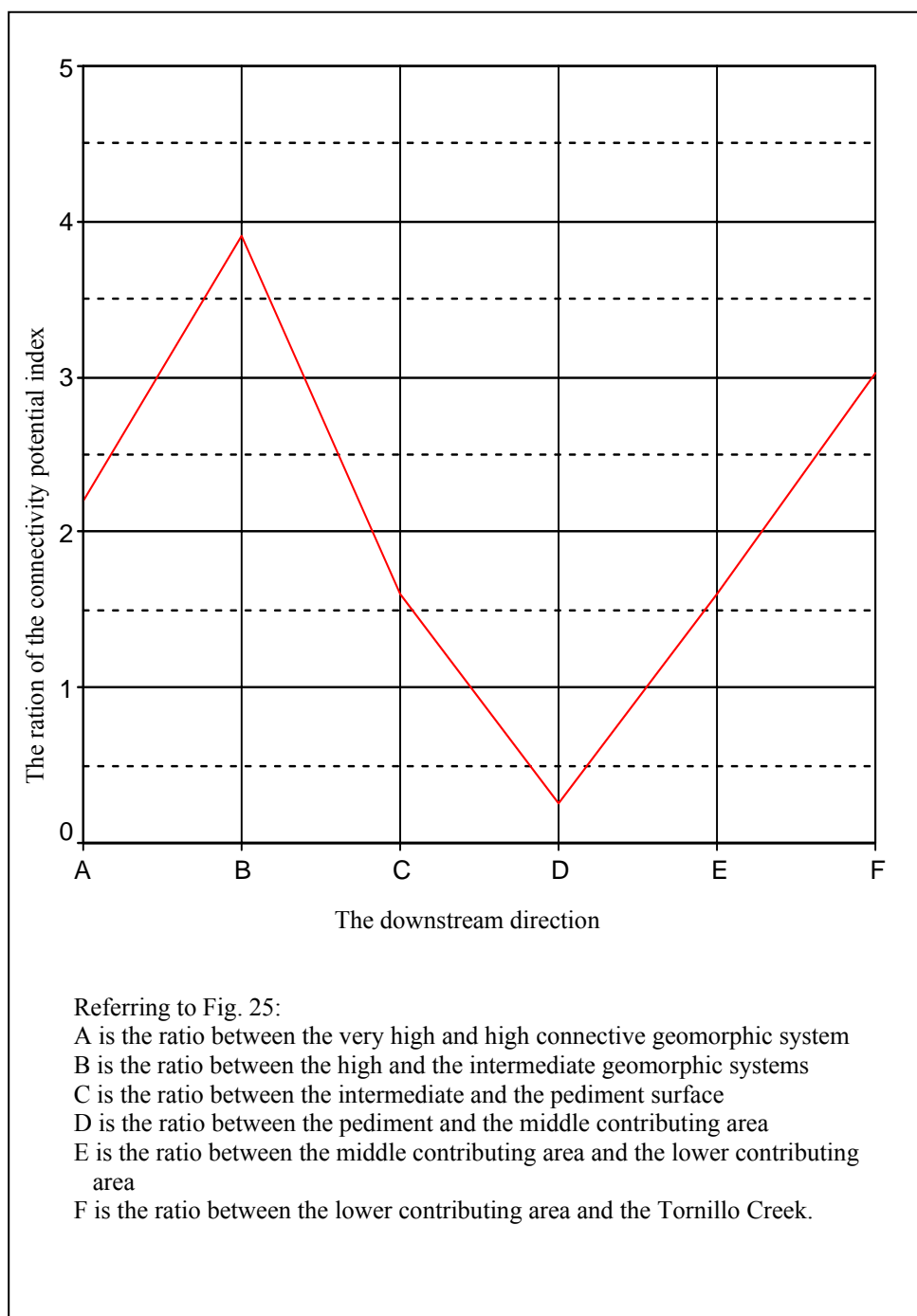


Fig. 28: The interaction between various geomorphic systems in Estufa Canyon.

connective systems and the low connective systems of the surface of the alluvial deposits (Fig. 26). This change is attributed to the influence of the area of the alluvial deposits, which function to suppress mass movement from the upper contributing area. Accordingly, deposition is highly expected to occur in the area of the alluvial deposits. However, the lowest ratio that occurs between the geomorphic systems of the area of the alluvial deposits and the middle contributing area allow alternative nature of the area of the alluvial deposits. The low ratio implies that the potential energy of the geomorphic systems in the middle contributing area is higher than the potential energy of the geomorphic systems in the area of the alluvial deposits. The increase in potential energy from the area of the alluvial deposits to the middle contributing area results in a maximization of mass movement in the area of the alluvial deposits. This process enhances the erosional nature of the area of the alluvial deposits. The erosional nature of the area of the alluvial deposits is shown by the absence of alluvial fans and bajadas. This nature, in turn, increases the stream power for transporting mass from the upstream geomorphic systems in the downstream direction. The overall result is high system connectivity between the upstream geomorphic systems in the western part of the study area and the geomorphic systems of the middle contributing area through a transitional erosional surface in the area of the alluvial deposits. This high system connectivity is supported as well by the high ratios between the middle contributing area and the lower contributing area (E), and, finally between the lower contributing area and Tornillo Creek (F). These ratios considerably exceed unity indicating high rates of transportation in the lower contributing area. The limited occurrence of the alluvial deposits along the

lower reach of the trunk stream supports the dominance of the transportation processes over the depositional processes in the lower contributing areas. The dominance of the transportation in the lower contributing area is expected to maintain the low ratio between the middle contributing area and the area of the alluvial deposits resulting in an overall high system-wide connectivity in Estufa Canyon.

CHAPTER VI

CONCLUSION AND FUTURE DIRECTIONS

Conclusion

One fundamental aspect of Earth's surface systems, in general, and of the geomorphic systems, in particular, is the interconnection between these systems. The interconnection between these systems has received intensive focus from researchers for a considerable time. In geomorphology, the interconnection between these numerous systems has been studied from various themes. The main two themes that received considerable attention are the mechanism of the connection between various geomorphic systems and the role of the connection in the landscape. The first theme pays particular attention to the spatial links by which the various geomorphic systems are linked. The second theme basically focuses on the process interrelationships between various geomorphic systems in response to external perturbations. Both themes have been studied through various conceptual frameworks introduced by geomorphologists. These concepts include process linkage (Ritter et al. 2002), complex-response (Schumm 2003), and coupling (Brunsden and Thornes 1979). These concepts basically, focus on the process interrelationship between geomorphic systems in response to changes in the external forces such as climate, tectonic, and sea level changes. Few studies have been carried out to provide a conceptual framework for studying the mechanism by which geomorphic systems are spatially linked. The above-mentioned concepts and studies provide a theoretical framework for studying the connectivity between the geomorphic systems. Unfortunately, none of these studies provided a developmental methodology

for studying the connectivity phenomenon between the geomorphic systems especially at the scale of the fluvial system.

In this dissertation, the connectivity concept between various geomorphic systems has been approached from a different perspective by defining and mapping the connectivity potential of various geomorphic systems. In this view, the connectivity potential is defined as the potential of a geomorphic system to transport mass to another geomorphic system. The influence of the connectivity potential of various geomorphic systems on the system-wide connectivity of the fluvial landscape was evaluated. To develop this approach, various objectives were established to studying the connectivity potential of geomorphic systems in the fluvial landscape. These objectives include mapping geomorphic systems that compose the fluvial landscape. The mosaiked image of six Digital Orthophotos Qaudrangle (DOQ) that include the study area was used along with the slope and lithology of the study area to identify various geomorphic systems. The second objective was extracting the landscape gradient of the study area. The landscape gradient represents the slope of the study area. It was extracted from a Digital Elevation Model of 30 m spatial resolution using the Slope Operation of the Spatial Analyst module available in ARCVIEW[®] GIS. The third objective was producing an image of the radar backscattering coefficient of the study area. The radar backscattering coefficient reflects the various roughness surfaces that cover various slopes in the study area. Both the landscape gradient and the surface roughness are raster layers that represent a continuous-scaled data that can be integrated using various GIS operations. The fourth objective was integrating both the landscape gradient and the surface

roughness to produce a raster layer that represents an index of the connectivity potential in the study area. This integration was carried out by multiplying the slope layer and the surface roughness layer using Map Algebra facility of the Spatial Analyst module of available ARCVIEW®. The higher the index values indicate higher values of slopes and surface roughness and then high potential energy for mass movement. The lower index values indicate low slope and low surface roughness and then low potential energy for mass movement. The raster layer that represents the Connectivity Potential Index (CPI) was used to perform the fifth objective.

In the fifth objective, raster vector GIS layers integration was carried out to calculate the mean of the connectivity potential index of each geomorphic system from the raster layer of the connectivity potential index. Calculating the mean of the connectivity potential index for each geomorphic system was performed by using the Summarize Zone Statistic operation of the Spatial Analyst module available in the ARCVIEW® GIS. The sixth objective of defining and mapping the connectivity potential of geomorphic systems was to identify patterns between means of the connectivity potential indices of geomorphic systems. The Natural Break classification method of ARCVIEW® GIS was used to classify the geomorphic systems according to their mean values of the connectivity potential index. In this methods, geomorphic systems can be classified into, geomorphic systems of low connectivity potential, geomorphic systems of intermediate connectivity potential and geomorphic systems of high connectivity potential. The last objective of the study was to evaluate the wide system connectivity of the fluvial landscape. To evaluate the system-wide connectivity,

the ratio between the connectivity potential of various classes of the connected geomorphic systems were calculated in the downstream direction. Thus, the ratio between the values of the connectivity potential of the upstream geomorphic systems (CPI_u) and the values of the connectivity potential of the downstream geomorphic systems (CPI_d) were estimated. These ratios produce three states: ratios that are greater than unity, ratios that approach unity and ratios that are less than unity. Evaluating these ratios helps define the process interrelationship between various geomorphic systems in the fluvial landscape and an overall evaluation of the dynamic setting of the fluvial landscape. These objectives were developed for studying the connectivity potential of geomorphic systems in Estufa Canyon, Big Bend National Park.

In Estufa Canyon, based on the values of the mean of the connectivity potential index, the geomorphic systems were classified into three main classes: geomorphic systems of low connectivity potential, geomorphic systems of intermediate connectivity potential, and geomorphic systems of high connectivity potential. The geomorphic systems of low connectivity potential are characterized by the lowest values of slopes and surface roughness. These systems occur in the area of the alluvial deposits in the middle of the study area. The geomorphic systems of high connectivity potential have the highest values of surface roughness and landscape gradient. These systems occur in the western part of the study area. The geomorphic systems of the intermediate values of the connectivity potential index occupy the middle and the lower contributing areas of Estufa Canyon. These systems occur as well between the high connective geomorphic systems in the western part and the geomorphic systems of the alluvial deposits of low

connectivity potential. The connectivity potential index of each geomorphic system can be used in understanding system-wide connectivity for the whole fluvial system of Estufa Canyon.

The system-wide connectivity is a concept that helps in the understanding of the process interrelationship between various geomorphic systems in the landscape. In this concept, a change in the potential energy of geomorphic systems results in maximizing or minimizing the mass movement of the contiguous geomorphic systems. The system-wide connectivity can help disclose whether mass movement between the geomorphic systems is in equilibrium or not. To study these relationships between various geomorphic systems, the ratio between the connectivity potential index of the upstream geomorphic system (CPI_u) and the connectivity potential index of the downstream geomorphic system (CPI_d) was calculated for the main geomorphic systems in the study area. Ratios that are higher than unity represent the presence of geomorphic systems that have high potential energy to transport mass in the downstream direction. Ratios that are less than unity indicate the presence of geomorphic systems that have high potential to produce headward erosion. These systems maximize mass transportation in the upstream geomorphic systems along with their high potential to transport mass in the downstream direction. The presence of these geomorphic systems in the upstream geomorphic systems of the fluvial system results in maintaining the erosional and transportational processes in the fluvial system. Ratios that approximate unity indicate the presence of equilibrium status between the contiguous geomorphic systems in the fluvial system.

In the study area, the geomorphic systems of high connectivity potential in the western part of the study area function to transport mass at high rates. In the eastward direction, the intensity of mass transportation decreases because of the presence of the alluvial deposits. However, the area of the alluvial deposits in the study area is not dominated by depositional geomorphic processes. The low ratio between the connectivity potential of the area of the alluvial deposits and the connectivity potential of the middle contributing area indicates a dynamic nature of the area of the alluvial deposits. The ratio indicates that the middle contributing area with its high connectivity potential index functions to maximize mass transportation on the surface of the alluvial deposits. The erosional nature of the area of the alluvial deposits is supported by the absence of alluvial fans and bajads. The dynamic nature of this area, in turn, would result in maximizing the connectivity potential of the geomorphic systems in the western part of the study area. Studying geomorphic systems from this perspective provides the capability for the geomorphologists, ecologists, and environmental scientists to predict the future behavior of the landscape for future landscape management.

Future Directions

The connectivity between various geomorphic systems in the landscape is a new area for research in geomorphology. This dissertation can be considered a fundamental document for various future directions to study the landscape from various perspectives.

Based on this study, an important new field that can be extended is the temporal changes in the connectivity potential of various geomorphic systems in the landscape.

This extension could provide the ability to predict changes in the connectivity potential of various geomorphic systems over various time scales. The notion of studying the temporal changes of the spatial links is critical for establishing short-term, medium-term and long-term developmental projects.

Studying the connectivity potential of various geomorphic systems in a landscape can be highly significant for environmental studies. Studying the connectivity potential between geomorphic systems could help determine the possible response of geomorphic systems against environmental perturbations. The fluvial system with high system-wide connectivity is expected to respond at higher rates against the external perturbations than the fluvial system that has low system-wide connectivity.

The current study provided a methodology for analyzing the connectivity between geomorphic systems as a function of two variables: the landscape gradient and the surface roughness. Other variables such as geology, vegetation, and soil moisture could be integrated together to establish a more extensive model that efficiently expresses the connectivity potential between various geomorphic systems.

The study discloses the possibility of the integration of satellite data with quantitative topographic data. An efficient quantitative remote sensing application for understanding the connectivity potential is possible by various satellite imageries such as LIDAR and GRACE remote sensing data. Both of the data can help quantify horizontal and vertical mass movement. Quantifying these movements, temporally and spatially, will help in better understanding the connectivity potential in the landscape.

Mapping surface roughness in Estufa Canyon using Radarsat-1 imagery indicates the possibility of using remote sensing imageries in remote areas on Earth. One of the possible applications is using the radar imageries in planetary studies. For instance, surface roughness of Mars can be mapped using radar imageries where the centimeter-scaled particle sizes can be mapped using these data.

REFERENCES

- Brown, S. R., 1987. A note of the description of surface roughness using fractal dimension. *Geophysical Research Letter* 14, 1095 – 1098.
- Brunsdon, D., 1993. Barriers to geomorphological change. In: Thomas, D. S. G., Allison, R. J. (Eds.), *Landscape Sensitivity*. Wiley, Chichester, U.K., pp 7 – 12.
- Brunsdon, D., Thornes, J. B., 1979. Landscape sensitivity and change. *Transactions of the Institute of the British Geographers* 4, pp 463 – 484.
- Bryan, K. 1973. Erosion and sedimentation in the Papago Country, Arizona. In: Schumm, S. A., Mosley, M. P. (Eds.), *Slope Morphology (Benchmark Papers in Geology)*, Dowden, Hutchinson & Ross, Inc., Stroudsburg, Pennsylvania pp 146 – 160.
- Canada Center of Remote Sensing 2004. Remote Sensing Tutorial. Natural Resources Canada.
- Chorley, R. J., 1962. Geomorphology and general system theory. *Geological Survey Professional Paper* 500 – B, pp B1 – B10.
- Chorley, R. J., Kennedy, B. A., 1971. *Physical Geography: A System Approach*. Prentice Hall International Inc., London.
- Church, M. 1992. Channel morphology and typology. In: Calow, P. Petts, G. E. (Eds.), *The River Handbook: Hydrological and Ecological Principles*, Blackwell Scientific Publications, Boston, pp 126 – 143.

- Croke, J., Mockler, S., Fogarty, P., Takken, I., 2005. Sediment concentration in runoff pathways from a forest road network and the resultant spatial pattern catchment connectivity. *Geomorphology* 68, pp 257 - 268.
- Dickerson, P. W. 1980. Structural zone transecting the Rio Grande Rift; preliminary observations. In: Dickerson, P. W., Hoffer, J. M., Callender, J. C. (Eds.). *Trans-Pecos Region; Southeastern New Mexico and west Texas*. New Mexico Geological Society 31, pp 63 - 70.
- Drury, S., 2001. *Image Interpretation in Geology*. Blackwell Science Inc., Malden, MA.
- Etzelmuller, B., 2000. On the quantification of surface changes using grid-based Digital Elevation Models (DEMs). *Transactions in GIS* 4(2), 129 – 143.
- Etzelmuller, B. Suleback, J. R., 2000. Developments in the use of the digital elevation models in periglacial geomorphology and glaciology. *Physische Geographie* 41, 35 – 58.
- Fukuda, S., Hirosawa, H. 1998. Suppression of speckle in synthetic aperture radar images usng wavelets. *International Journal of Remote Sensing* 19, 507 – 519.
- Gilvear, D. J., 1999. Fluvial geomorphology and river engineering: future roles utilizing a fluvial hydrosystems framework. *Geomorphology* 31, 229 – 245.
- Goodman, J. W., 1976. Some fundamental properties of speckle. *Journal of the Optical Society of America* 66, 1145 – 1150.
- Goudie, A. S., 1997. Weathering processes. In: Thomas, D. S. G. (Ed.), *Arid Zone Geomorphology: Process, Forms, and Change in Drylands*, John Wiley & Sons, New York, pp 25 – 39.

- Hugget, R. J., 1985. *Earth Surface Systems*. Springer-Verlag, New York.
- Harvey, A. M., 1994. Influence of slope/stream coupling on process interactions on eroding gully slopes: Howgill Fells, northwest England. In: Kirkby, M. J. (Ed.), *Process Models and Theoretical Geomorphology*. Wiley, Chichester, U.K., pp 247 – 270.
- Harvey, A. M., 2001. Coupling between hillslopes and channels in upland fluvial systems: implications for landscape sensitivity, illustrated from the Howgill Fells, northwest England. *Geomorphology* 42, 255 – 250.
- Humphrey, N. F., Heller, P. L., 1995. Natural oscillations in coupled geomorphic systems: an alternative origin for cyclic sedimentation. *Geology* 23, 449 – 502.
- Jones, A. P., 2000. Late Quaternary sediment sources, storage and transfers within mountain basins using clast lithologic analysis: Pineta Basin, central Pyrenees, Spain. *Geomorphology* 34, 145 – 161.
- Lancaster, N., Nickling, W. G., Neuman, M. C., 2002. Particle size and sorting characteristics of sand in transport on the stoss slope of a small reversing dune, *Geomorphology* 43 (3 – 4), 233 – 242.
- Laszlo, E. 2003. *The Connectivity Hypothesis: Foundations of an Integral Science* Quantum, Cosmos, Life, and Consciousness. State University of New York Press, Albany.
- Lawson, A. C., 1915. *The epigene profiles of the desert*. University of California Publications in Geological Sciences, University of California. Berkeley, pp 23 – 48.

- Lehman, T. M., 1991. Sedimentation and tectonism in the Laramide Tornillo basin of west Texas. *Sedimentary Geology* 75, 8 – 28.
- Lewis, A. J., Henderson, F. M., 1998. Radar fundamentals: the geoscience perspective. In: Henderson, F. M., Lewis, A. J. (Eds.), *Principles & Applications of Imaging Radars, Manual of Remote Sensing*, John Wiley & Sons, Inc., New York, pp 131 – 181.
- Lopes, A. Nezry, E., Touzi, R., Laur, H. 1993. Structure detection and statistical adaptive speckle filtering in SAR images. *International Journal of Remote Sensing* 4(9), pp 1735 – 1758.
- Ludwig, J. A., Muldavin, E., Blanche, K. R., 2000. Vegetation change and surface erosion in desert grasslands of Otero Mesa, southern New Mexico: 1982 to 1995. *The American Midland Naturalist* 144, pp 273 – 285.
- Mark, D. M., 1975. Geomorphometric parameters: a review and evaluation. *Geografiska Annaler* 57a, 157 – 177.
- Maxwell, R. A., Lonsdale, J. T., Hazzard, R. T., Wilson, J. A., 1967. *Geology of Big Bend National Park, Brewster County, Texas*. Bureau of Economic Geology. The University of Texas at Austin.
- Muehlberger, W. R., 1980. Texas lineament revisited: in the Trans-Pecos region, southeastern New Mexico of west Texas. In: Dickerson, P. W., Hoffer, J. M., (Eds.), *New Mexico Geological Society Guidebook: Trans-Pecos Region*, pp 113 – 121.
- Parsons, A. J. 1988. *Hillslope Form*. Routledge, New York.

- Parsons, A. J., Abrahams, A. D., Simanton, J. R., 1992. Micro-topography and soil surface materials on semi-arid pediment hillslopes, southern Arizona. *J. Arid Environ.* 22, 107 – 115.
- Peake, W. H., Oliver, T. L., 1971. The response of terrestrial surface at microwave frequencies. Ohio State University Technical Report 2440-7, Columbus, Ohio.
- Phillips, J. D., 1992. The end of equilibrium. *Geomorphology* 5, 195 – 201.
- Phillips, J. D., 1999. *Earth Surface Systems: Complexity, Order, and Scale*. Blackwell Publishers Inc, Malden, Massachusetts.
- Pike, R. J., Rozema, W. J., 1975. Spectral analysis of landforms. *Annals of the Association of American Geographers* 85 (4), 499 – 516.
- Plumb, G. A., 1992. Vegetation classification of Big Bend National Park, Texas. *The Texas Journal of Science* 44 (4), 375 – 387.
- Poole, G. C., Stanford, J. A., Frissel, C. A., Running, S. W., 2002. Three dimensional mapping of geomorphic controls flood plain hydrology and connectivity from aerial photos. *Geomorphology* 48, 329 – 347.
- Radarsat International 1997. RADARSAT Curriculum Guideline. Available at <http://www.rsi.ca/rsic/education/rghb.pdf>.
- Ritter, D. E., Kochel C. R., Miller, J. R. 2002. *Process Geomorphology*, 4th Ed. McGraw – Hill, Boston.
- Schlesinger, W. H., Abrahams, A. D., Pearson, A. J., Wainright, J., 1999. Nutrient losses in runoff from grasslands and shrubland habitats in southern New Mexico: I. Rainfall simulation experiment. *Biogeochem.* 45, 21 – 34.

- Scholz, E., 1972. The construction of morphographic and morphometric maps. In: Demek, J. (Ed.), Manual of detailed geomorphological mapping. Academia, Publishing House of the Czechoslovak Academy of Sciences, Prague.
- Schumm, S. A., 2003: The Fluvial System. The Blackburn Press, Caldwell, New Jersey.
- Shaber, G. G., Berlin, G. L., Brown, W. E., 1976. Variations in surface roughness within Death Valley, California: geologic evaluation of 25-cm wavelength radar images. Geologic Society of America Bulletin 87, 29 – 41.
- Shepherd, N. 1997. Extraction of beta nought and sigma nought from radarsat CDPF products. Report No. AS97 – 5001, 30 spe 1997, Canadian Space Agency, Ottawa, Canada.
- Soil survey of Big Bend National Park, Part of Brewster Country 1985. United States Department of Agriculture, Texas.
- Stevens, J. B., Stevens, M. S., 1985. Basin and range deformation and depositional timing, Trans-Pecos, Texas. In: Dickerson, P. W., Muehlberger, W. R. (Eds.), Structure and Tectonic of Trans-Pecos, Texas. West Texas Society Field Conference, Publications 85 – 81, pp 231 - 234.
- Thurwachter, J. E., 1984. Sedimentology of Neogene basin-fill deposits, lower Tornillo Creek area, Big Bend National Park, Teaxs. M.S. Thesis, The University of Texas at Austin.
- Udden, J. A., 1907. A sketch of the geology of the Chisos country, Brewster County, Texas. University of Texas Bulletin 93, p 101.

- Ulaby, F. T., Moore, R. K., Fung, A. K., 1982. Microwave Remote Sensing: Active and Passive, Vol. II, Remote Sensing and Surface Scattering and Emission Theory. Addison – Wesley Publishing Company, Reading, Massachusetts.
- Von Bertalanffy, L., 1956. General System Theory. General Systems Year Book, Ann. Arbor., Michigan, 4.
- Wall, S. D., Farr, T. G. 1991. Measurements of surface microtopography. Photogrammetric Engineering and Remote Sensing 57 (8), 1075 – 1078.
- Wilson, J. A., 1959. Transfer, a synthesis of stratigraphic processes. American Association of Petroleum Geologists Bulletin 43, pp 2861 – 2862.
- Wondzell, S. M., Ludwig, J. A., 1995. Community dynamics of desert grasslands: influence of climate, landforms, and soils. Journal Vegetation Sciences 6, 377 – 390.
- Xiao, J., Li, J., Moody, A. 2003. A detail preserving and flexible adaptive filter for speckle suppression in SAR imagery. International Journal of Remote Sensing 24(12), 2451 – 2465.

VITA

Name: ElSayed Ali Hermas Ibrahim

Address: Texas A&M University
Geology & Geophysics Department
College Station, TX 77843 – 3115

E-mail Address: eahermas@gmail.com

Education: B.S., 1986, Geology and Geochemistry, Faculty of Science
Mansoura University, Egypt

M.S., 1992, Geology, Faculty of Science
Mansoura University, Egypt

Position: Assistant Researcher
Department of Geology and Mineral Resources
The National Authority of Remote Sensing and Space Science
(NARSS)
Cairo, Egypt